

1 **Prediction of response to anti-cancer drugs becomes robust via**  
2 **network integration of molecular data**

3 Marcela Franco<sup>1</sup>, Ashwini Jeggari<sup>2</sup>, Sylvain Peugot<sup>1</sup>, Franziska Böttger<sup>1,3</sup>, Galina Selivanova<sup>1</sup> and Andrey  
4 Alexeyenko<sup>1,4\*</sup>

5 <sup>1</sup> Department of Microbiology, Tumor and Cell Biology (MTC), Karolinska Institutet, Stockholm, Sweden.

6 <sup>2</sup> Department of Cell and Molecular Biology, Karolinska Institutet, 171 77 Stockholm, Sweden.

7 <sup>3</sup> Present Address: OncoProteomics Laboratory, Department of Medical Oncology, VU University Medical  
8 Center, 1081HV Amsterdam, The Netherlands

9 <sup>4</sup> National Bioinformatics Infrastructure Sweden, Science for Life Laboratory, Box 1031, 17121, Solna,  
10 Sweden

11

12 \* To whom correspondence should be addressed. Tel: +46 8 52481513; email:

13 [andrej.alekseenko@scilifelab.se](mailto:andrej.alekseenko@scilifelab.se); address: SciLifeLab, Box 1031, 171 21 Solna, Sweden

14

15

16

## 17 ABSTRACT

18 In order to tackle heterogeneity of cancer samples and high data space dimensionality, we propose finding  
19 sensitive and robust biomarkers at the pathway level. Scores from network enrichment analysis transform  
20 the original space of altered genes into a lower-dimensional space of pathways, which is then correlated with  
21 phenotype variables. The analysis was first done on *in vitro* anti-cancer drug screen datasets and then on  
22 clinical data. In parallel, we tested a panel of state-of-the-art enrichment methods. In this comparison, our  
23 method proved superior in terms of 1) universal applicability to different data types with possibility of cross-  
24 platform integration, 2) consistency of the discovered correlates in independent drug screens, and 3) ability  
25 to explain differential survival of patients. Our new screen validated performance of the discovered  
26 multivariate models. Only the network-based method could discover markers that predict both response *in*  
27 *vitro* and patient survival given administration of the same drug.

28

## 29 List of abbreviations

- 30 • AGS, altered gene set (gene set characterizing an individual sample/cell line/patient);
- 31 • FGS, functional gene set (typically a pathway);
- 32 • NEA, network enrichment analysis;
- 33 • PWNEA, NEA at pathway level (i.e. by using multi-gene FGS);
- 34 • GNEA, NEA by using single-gene FGS (i.e. individual network nodes);
- 35 • ORA, overrepresentation analysis of FGS versus AGS;
- 36 • GSEA, gene set enrichment analysis of FGS versus full ranked gene lists;
- 37 • AGSEA, variant of GSEA where genes are ranked by absolute value;
- 38 • ZGSEA, variant of GSEA where genes are ranked by z-score of deviation from cohort mean.

39

40

## 41 INTRODUCTION

42 The problem known as the “dimensionality curse” (Bittner, 1962),(Heng, 2015) - when a set of few (tens to  
43 hundreds) biomedical samples are described with a much larger number of molecular variables - undermines  
44 robustness of phenotype predictors. This was aggravated further when novel omics platforms expanded the  
45 variable space from thousands to nearly millions of potentially informative molecular features. In addition,  
46 profiling of cancer samples revealed that genomic alterations across tumors of the same type appear  
47 disparate and poorly overlapping (Heng, 2015). As a result, variability between cancer samples is often  
48 higher than is assumed by the common parametric statistics (Lee et al., 2015). Beyond a few success cases  
49 (Parker et al., 2009),(Wang et al., 2005), molecular cancer signatures have been hard to corroborate in a  
50 novel, independent cohort. Across a number of meta-analyses, conclusions about practical applicability of  
51 the signatures range from entirely negative (Roepman et al., 2009),(J. Subramanian & Simon, 2010) to  
52 mixed or moderately positive (Waldron et al., 2014). The common understanding is that seemingly disparate  
53 individual events must be confluent to certain pathways that represent cancer hallmarks and pathways (Iorio  
54 et al., 2016).

55 When molecular landscapes of cancer cell lines were found to be very different from those of original tumors,  
56 modeling drug response *in vitro* was questioned (Domcke, Sinha, Levine, Sander, & Schultz, 2013). A later,  
57 more comprehensive exploratory analysis demonstrated overall consistence of molecular aberrations  
58 between cell lines and primary tumors from matching cancer sites (Iorio et al., 2016) – although these  
59 authors did not investigate the therapeutic relevance of discovered *in vitro* correlates. Haibe-Kains and co-  
60 authors published a discouraging comparison (Haibe-Kains et al., 2013) between two large *in vitro* screens  
61 (Barretina et al., 2012),(Garnett et al., 2012). After that conclusion and the following polemics (Stransky et  
62 al., 2015), the urgent need for cross-platform and clinically based validation became even more apparent. It  
63 is dictated by both statistical and biological challenges, such as excessive data dimensionality, imperfect  
64 analytical tools, the heterogeneity of cancer genomes, and the downstream diversity of methylation and  
65 expression patterns (Crystal et al., 2014). Authors of one of the most up-to-date investigations still admitted  
66 that the ability of cancer cell drug screens “to inform development of new patient-matched therapies...  
67 remains to be proven” (Seashore-Ludlow et al., 2015). On the clinical side, oncologists expected reports on  
68 patient-specific alterations in the light of knowledge available from computerized support systems (Kurnit et  
69 al., 2017). In our view, these challenges could be most systematically addressed by summarizing sparse,  
70 disparate events at the pathway level via the global interaction network.

71 Adding omics data to clinical variables has demonstrated the potential for prediction of cancer disease  
72 outcome in a DREAM challenge (Margolin et al., 2013). One particularly winning strategy was to employ  
73 multigenic expression patterns. Such 'meta-genes' (Cheng, Yang, & Anastassiou, 2013) were, despite the  
74 seemingly 'network-free' definition, nothing other than modules in a co-expression network, which allowed  
75 dimensionality reduction and a biological generalization. Another DREAM project revealed efficiency of  
76 summarizing gene expression in cancer cell lines over pathways (Costello et al., 2014).

77 Further, identifying patient sub-categories responsive to a treatment is more challenging than one-  
78 dimensional drug sensitivity or survival analyses. A practical method should secure feature profiles for each  
79 individual in the cohort, so that the profiles can be fit to clinical variables and covariates. Therefore, a crucial  
80 feature for biomarker discovery would be the ability to assign scores to individual samples rather than  
81 deriving feature-pathway associations from the whole data collection. In addition, further sample  
82 classification in a flow of new patients should not require re-running the analysis on the whole cohort, i.e.  
83 recalculating the data space, as is often the case.

84 In this work, we use acronym NEA to refer to a specific approach for network enrichment analysis, which  
85 ascends to the idea of accounting for the node degrees of individual genes. Maslov & Sneppen (2002)  
86 proposed an algorithm of systematic randomization of the network via swapping each edge of each node,  
87 which preserved topological properties of the network items. When implemented in NEA (Andrey  
88 Alexeyenko et al., 2012), this idea enabled characterization of experimental or clinical samples with pathway  
89 scores by accounting for genes' relationships in the global gene interaction network. The sample-specific  
90 pathway-level output was simple, uniform and statistically sound, so that it could be used in downstream  
91 analyses with arbitrary phenotype models. Due to the ability to summarize rare alterations that cause the  
92 recurrent cancer phenotypes, pathway profiles might provide more information on the underlying biology and  
93 could be more robust as predictors of clinical outcomes. The drawback of NEA was (beyond the long  
94 execution time required for network randomization) a bias in significance estimation for smaller gene sets.  
95 On the other hand, the high statistical power to detect such compact, specific sets would be the most salient  
96 feature of NEA. We therefore developed a fast, convenient, and unbiased implementation of the algorithm  
97 (Jeggari & Alexeyenko, 2017).

98 However neither NEA nor alternative methods of pathway enrichment had been systematically applied to the  
99 task presented above: the discovery of biomarkers suitable for individual outcome prediction.

100 In the first section of Results, we provide a detailed explanation of the NEA approach and an instructive  
101 example, which are both done in comparison with alternative methods. In order to select a representative set  
102 of such methods, we investigated a wide range of earlier proposed algorithms and approaches. Since they  
103 were mostly designed for purposes different from ours, their applicability was often limited. In Methods  
104 (section “Alternative Methods of Pathway and/or Enrichment Analysis”), we discuss their principles, consider  
105 both applicability to biomarker discovery and software usability, and thereby motivate our choice of methods  
106 presented in Figure 1 and Table 1. The outline and details of the comparative performance evaluation are  
107 then reported in Results. More specifically, we: 1) assess content of relevant information in three published  
108 experimental *in vitro* drug screens (Barretina et al., 2012) (Garnett et al., 2012) (Basu et al., 2013) (dubbed  
109 CCLE, CGP, and CTD, respectively), 2) investigate preservation of this content across drug screens and  
110 then in one novel dataset, 3) perform a novel, small scale drug screen and demonstrate that the pathway-  
111 level multivariate models withstand the independent validation, and finally 4) validate the identified  
112 correlations in clinical treatment profiles from TCGA (Cancer Genome Atlas Research Network, 2008) (Table  
113 2). The performance of our method in these analyses is measured in parallel with using original gene profiles  
114 and the alternative enrichment methods of ORA, GSEA (in two versions), and SPIA (Fig. 1; Table 1).

## 115 RESULTS

### 116 1. Background

117 The main principle of NEA can be understood via comparison to gene set enrichment analysis in its simplest  
118 form, the so called overrepresentation analysis (ORA) (Huang, Sherman, & Lempicki, 2009) (Fig. 1A). An  
119 experimental or clinical sample can be characterized by a set of altered genes (AGS), such as top ranking  
120 differentially expressed genes, or a set of somatic mutations, or a combination of these. The other  
121 component of the analysis is a collection of functional gene sets (FGS): pathways, ontology terms, or custom  
122 sets of biological importance. Importantly, FGS collections should represent existing knowledge, being either  
123 expert curated or derived from experimental data. Enrichment scores of the AGSs can thus be used as the  
124 samples' coordinates in the lower-dimensional FGS space. In ORA, enrichment is measured by the number  
125 of genes shared by the FGS and the AGS, given the sizes of the latter. NEA considers the network  
126 environment by counting the **network edges that connect** any genes of AGS with any genes of FGS (Fig.  
127 1D). In both ORA and NEA significance can be evaluated with appropriate statistical tests. For NEA, this  
128 evaluation must be additionally normalized by accounting for topological properties of the network nodes.  
129 Due to the presence of different interaction mechanisms in the global network, NEA does not expect FGS

130 genes to be altered themselves and therefore is capable of detecting enrichment of e.g. a transcriptomics  
131 based AGS in a pathway that operates by other mechanisms, such as trans-membrane signaling,  
132 phosphorylation etc. Compared to ORA, NEA holds other key advantages, such as exceptionally high power  
133 to detect enrichment in a global network, given the latter is sufficiently dense, i.e. when the median number  
134 of edges per gene is around 50. Hence, even smaller gene sets often connect to each other by multiple  
135 edges. An ultimately reduced FGS can even appear as an individual key network node. This gene-level  
136 network analysis, GNEA (Fig. 1E) provides a more focused alternative to the default analysis at the pathway  
137 level, PWNEA (Fig. 1D) and we therefore separately evaluate performance of PWNEA and GNEA in the  
138 present work.

139 Figure 1. Rendering biological samples into pathway space with alternative enrichment methods.

140 The placement of three cancer cell lines HuH-7, NCI-H684, and RT-112 in a 2-dimensional space of pathways 'PPAR signaling'  
141 and 'WNT signaling' (KEGG#03320 and KEGG#04310) (A, B, C, and D) or, alternatively, in a space of two key genes from these  
142 pathways (E) was done by using cell line-specific altered gene sets, AGS, which originated from transcriptomics data and  
143 contained 226, 143, and 48 member genes, respectively (AGS of class `significant.affymetrix_ccle`, see details in  
144 Methods).

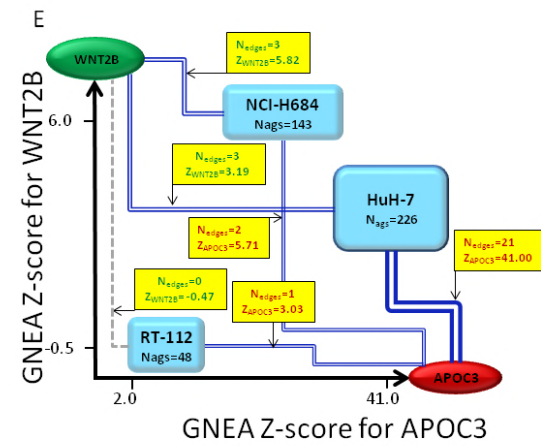
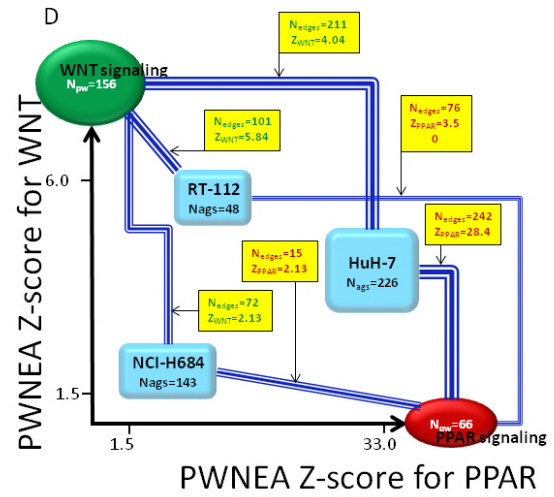
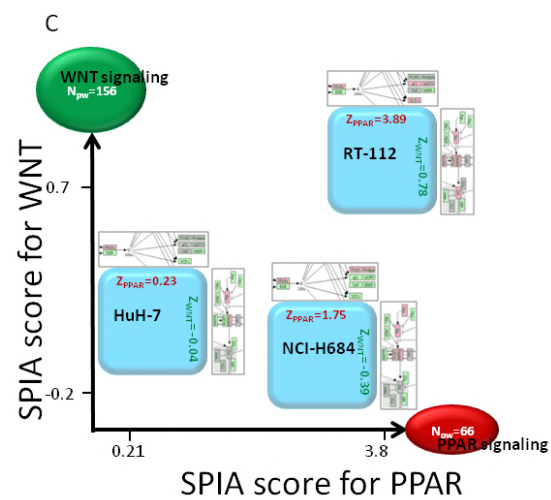
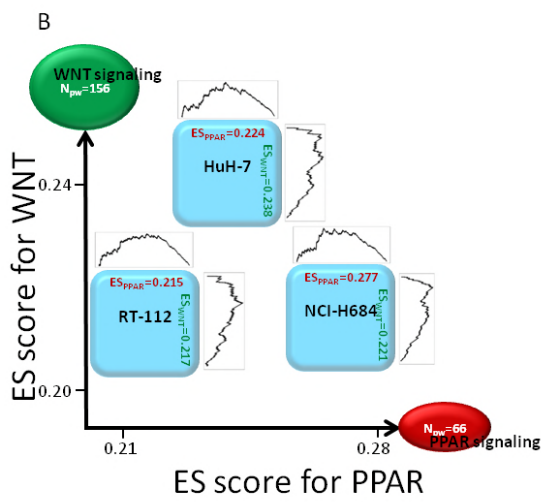
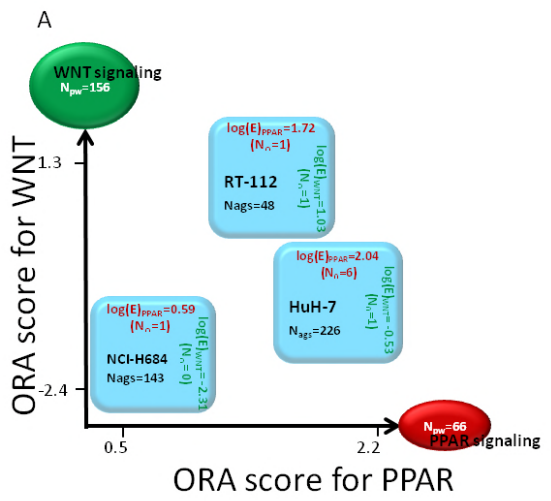
145 A. ORA: enrichment of the three AGSs was analyzed against the two pathways (or, more generally, functional gene sets, FGS)  
146 using the overrepresentation analysis. The pathway enrichment scores were calculated from overlap between the gene sets.  
147 For clarity we here denote the pathway size  $N_{PW}$  which corresponds to  $N_{FGS}$  elsewhere in the article. Due to the relatively small  
148 gene sets sizes ( $N_{PW}$  and  $N_{AGS}$ ), a noticeable ( $N_{\cap} > 1$ ) and significant overlap was observed in just one out of six cases, which  
149 could limit the ORA sensitivity.

150 B. GSEA was calculated using the full ranked gene lists from each cell line sample (A. Subramanian et al., 2005).

151 C. SPIA accounted for topological relationships of altered genes within the pathways. More weight was assigned to patterns of  
152 consistent up/down-regulation, i.e. where deregulated genes adjoined in regulatory cascades. Relatively disjoint regulatory  
153 events contributed with lower weights. The gene set submitted to SPIA can be of arbitrary size, up to full length, as in GSEA.  
154 The fold change values determine relative influence of the pathway genes.

155 D. NEA: the coordinates of the three AGSs in the space of two pathways were determined via network enrichment analysis. The  
156 NEA z-scores (on the axes and in yellow boxes) were calculated via network connectivity rates between corresponding AGS and  
157 FGS by taking into account the numbers of AGS-FGS links ( $N_{edges}$  in yellow boxes) and the node topology of the member genes  
158 (Fig. 1 and Methods). The summarized connections between AGSs and FGSs are shown by blue compound edges that  
159 represent multiple individual gene-gene edges in the global network ( $N_{edges}$ ). Individual edges within AGSs and within FGSs are  
160 not used in the analysis.

161 E. GNEA: since the power of NEA to detect network enrichment was high, it was possible to apply NEA to the cell line AGSs  
162 versus individual gene network nodes WNT2B and APOC3 in the same way as it was done versus pathways in D. Even though  
163 the  $N_{edges}$  values were expectedly smaller than in B, four out of six Z-scores appeared rather high.



164

165

166 Table 1. Characteristic features of the alternative methods.

Method	Type of input data	Allows data type integration	Level of input (samples)	Network analysis	Level of output (features)
original profiles	Any	-	All genes	-	[same as input]
ORA	Any	+	Altered gene sets	-	Functional gene sets
AGSEA	Expression	-	All genes	-	Functional gene sets
ZGSEA	Expression	-	All genes	-	Functional gene sets
SPIA	Expression	-	All genes	+	Functional gene sets
PWNEA	Any	+	Altered gene sets	+	Functional gene sets
GNEA	Any	+	Altered gene sets	+	Network gene nodes

167

168 Thus, each of the methods in Figure 1 enables quantitative characterization of individual samples, although  
 169 they may differ in input, processing, and output (Table 1). Further, the data analysis procedure included the  
 170 following steps: 1) characterization of each sample/patient with either full gene profile or a limited-length  
 171 altered gene set (AGS) obtained via analysis of the genome, transcriptome etc., 2) enrichment analysis  
 172 (except the option "original profiles") against the functional gene sets, FGS, which rendered the analyzed  
 173 samples into the  $N_{FGS} \times N_{AGS}$  space, and 3) phenotype modeling by using either the original gene profiles or  
 174 FGS profiles in the same way (not shown in Table 1; see Methods for details). In order to maximally adapt  
 175 GSEA to our applications, we tested two different ways of ranking gene lists, AGSEA and ZGSEA (*Methods*)  
 176 and present respective results separately.

177 In sections 3..5 of Results, we report the results of systematic analyses of the experimental datasets with  
 178 the alternative methods in order of increasing complexity (Table 2).

179 Table 2. Steps of analysis using alternative methods from Table 1.

180

Step	What was evaluated	Figure	Scheme
1	Statistical power to detect correlates of drug sensitivity (fraction of significant correlates per dataset)	3	Within 3 published <i>in vitro</i> screens; within TCGA clinical datasets
2	Consistency of the discovered correlates between drug screens: cross-validation	4	Between 3 published <i>in vitro</i> screens
3	Consistency of multivariate models between drug screens: independent validation	5	From CTD <i>in vitro</i> screen to the novel ACT screen
4	Agreement between <i>in vitro</i> screens and clinical data	6	From 3 published <i>in vitro</i> screens to TCGA clinical datasets

181



182 We begin by introducing an example of data analysis and interpretation (Fig. 2). Using data from the CGP in  
183 vitro screen, we observed a negative correlation between the PWNEA scores for pathway KEGG#00670  
184 “One carbon pool by folate” for cell line AGS features `significant.affymetrix_ccle`, on the one hand,  
185 and sensitivity to methotrexate on the other hand (Spearman rank  $R = -0.248$ ;  $p(H_0) = 2.37e-06$ ). The  
186 relatively low magnitude of the correlation is typical of such analyses and was explained by minor fractions of  
187 responders among all tested genotypes (Stransky et al., 2015). We compared cell lines which combined  
188 lowest sensitivity to methotrexate with highest PWNEA scores for KEGG#00670 (dubbed here Drug-/PW+)  
189 versus those possessing highest sensitivity and lowest PWNEA scores (Drug+/PW-) (ten cell lines in each  
190 set). Figure 2 (A,B,D,E) displays the network connectivity of the FGS KEGG#00670 “One carbon pool by  
191 folate” with AGSs for two cell lines (MPP89, ECGI10) of group Drug-/PW+ and two cell lines (RS411, A2780)  
192 of group Drug+/PW-. As an example, MPP89 obtained an NEA score of  $Z=8.09$  (NEA FDR=4.3e-10; see  
193 details in Methods) because there were  $n_{AGS-FGS} = 19$  edges in the network between its AGS and the FGS,  
194 against  $\hat{n}_{AGS-FGS} = 4.89$  edges expected by chance, i.e. in a random network of the same degree  
195 sequence. For comparison, the NEA  $Z$ -score for A2780 was as low as  $-0.77$  and insignificant. The negative  
196 sign indicated that the number of network edges  $n_{AGS-FGS} = 10$  between the AGS and FGS was lower than  
197 the value expected by chance,  $\hat{n}_{AGS-FGS} = 12.54$ . The expected numbers  $\hat{n}_{AGS-FGS}$  differed between MPP89  
198 and A2780 due to the difference in the cumulative AGS degrees  $N_{AGS}=2268$  and  $N_{AGS}=5823$ , respectively  
199 (shown in Fig. 2F). The high score for MPP89 (Fig. 2A) was likely influenced by the network node of  
200 formimidoyltransferase cyclodeaminase FTCD, which provided 14 out of the 19 edges. Although enrichment  
201 against the same FGS might have been enabled via entirely different AGS member genes, we note that it  
202 was not the case here: FTCD was a member of four out of the ten AGS of the group Drug-/PW+.  
203 Methotrexate is a cytostatic drug that inhibits dihydrofolate reductase, thereby blocking synthesis of  
204 tetrahydrofolate, the downstream production of folic acid, and finally that of thymidine. We can therefore  
205 hypothesize that overexpression of FTCD, an enzyme controlling the interconversion between  
206 formimidoyltetrahydrofolate and tetrahydrofolate (Tabor & Wyngarden, 1959), might have rescued the  
207 thymidine production by supplying extra tetrahydrofolate (Rajagopalan et al., 2002). Since FDCD itself is a  
208 member of the “One carbon pool by folate”, the pathway could be, in principle, detected by another  
209 enrichment algorithm. But how have the alternative tested enrichment methods dealt with this pattern? Any  
210 noticeable correlations were absent. This might be explained by the fact that FDCD was the only consistently  
211 deregulated gene out of the whole pathway, which was a challenging situation for each of these methods.  
212 ORA is not well fit for cases of such an overlap ( $N=1$ ). In GSEA, enrichment via a single highly ranked list

213 member is usually not detectable. In its turn, SPIA could not gain enough statistical power in absence of  
214 consistent (adjoining) patterns of dysregulation in multiple genes. Finally, expression of FTCD itself did not  
215 significantly correlate with methotrexate sensitivity in CCLE and CGP transcriptomics datasets. More broadly,  
216 we did not find any genes of the “One carbon pool by folate” and the adjoining pathway KEGG#00790  
217 “Folate biosynthesis” which would significantly (by requiring q-value <0.05) correlate with methotrexate  
218 sensitivity at either gene expression or somatic mutation levels.

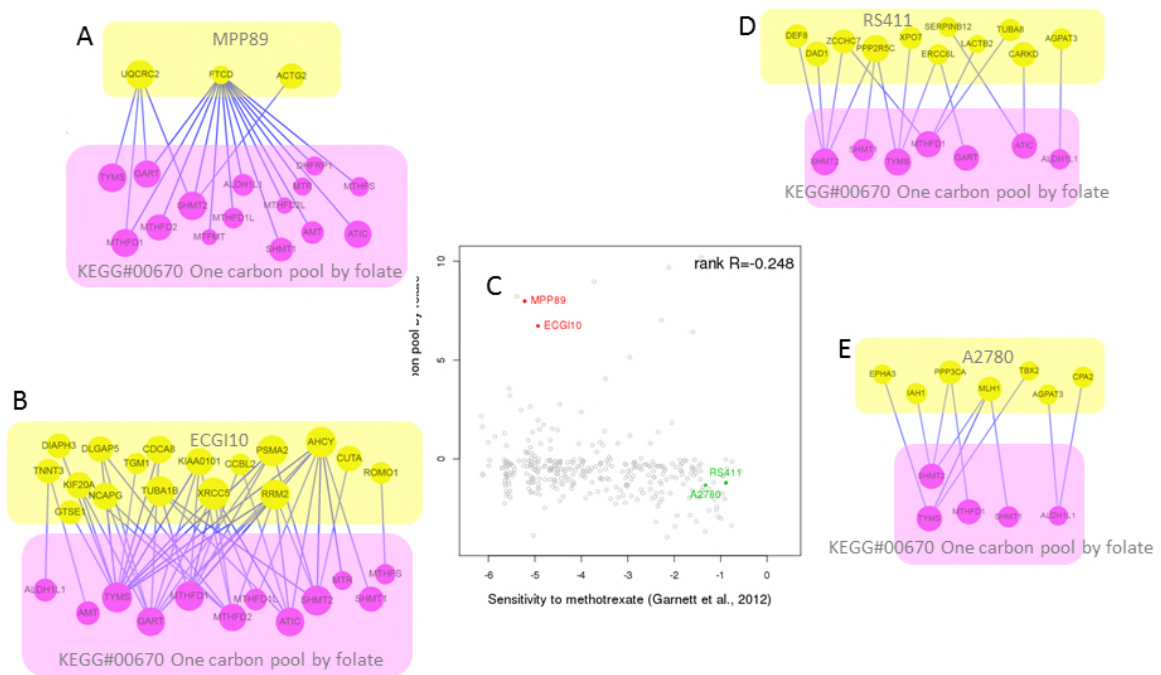
219 For comparison, AGS of the other resistant cell line, ECG110, did not share any genes with the target  
220 pathway (Fig. 2B), although still received a higher NEA score. In this case, the summarized connectivity was  
221 not dominated by a single network node of the AGS or of the FGS. Here the drug resistance could potentially  
222 have been mediated by the DNA repair protein XRCC5 or by the adenosylhomocysteine hydrolase AHCY,  
223 which were earlier reported to be implicated in methotrexate resistance (Snijders et al., 2008) and  
224 folate metabolism (Pogribny et al., 2017), respectively. Unlike the upregulated FTCD in MPP89,  
225 both these genes were strongly downregulated in ECG110. This emphasizes another feature of NEA: genes  
226 may be included into AGS due to alterations in an arbitrary direction, i.e. both over- and under-expression,  
227 hyper- and hypo-methylation, increased and decreased copy number etc. Therefore higher and, respectively,  
228 lower NEA scores cannot be traditionally interpreted as activation or suppression of the given pathway (FGS)  
229 but rather indicate a general 'pathway perturbation'. Hence the pathway “One carbon pool by folate” was  
230 unperturbed in the low-scoring cell lines A2780 and RS411, i.e. the latter did not exhibit features that could  
231 connect specifically to the pathway.

232

233 Figure 2 Network enrichment analysis of four cell line AGSs with differential response to methotrexate.

234 While using AGSs of class `significant.affymetrix_ccle`, the response of cancer cell lines to methotrexate in  
 235 CGP screen correlated with NEA scores (pane F) in regard to FGS “One carbon pool by folate” (pane C). The  
 236 methotrexate-resistant cell lines MPP89 and ECGI10 (panes A and B) received higher NEA scores since the numbers  
 237 of edges  $n_{AGS-FGS}$  connecting them to the FGS significantly exceeded those expected by chance,  $\hat{n}_{AGS-FGS}$  (52 vs  
 238 26.02 and 19 vs. 4.89, respectively; pane F). For comparison, the sensitive lines RS411 and A2780 (panes D and E)  
 239 had fewer edges than expected (15 vs 19.93 and 10 vs. 12.54, respectively) and therefore received lower, negative  
 240 scores.

241 The table in F and the sub-networks in A, B, D, and E were created via the web-site for interactive NEA  
 242 <https://www.evinet.org/>.



$$\chi^2 = \frac{(n_{AGS-FGS} - \hat{n}_{AGS-FGS})^2}{\hat{n}_{AGS-FGS}} + \frac{(!n_{AGS-FGS} - !\hat{n}_{AGS-FGS})^2}{! \hat{n}_{AGS-FGS}}; \quad \hat{n}_{AGS-FGS} = \frac{N_{AGS} * N_{FGS}}{2 * N_{total}}$$

F

AGS			FGS			Network enrichment analysis					ORA
Name	$N_{nodes}$	$N_{edges}$	Name	$N_{nodes}$	$N_{edges}$	$n_{AGS-FGS}$	$\hat{n}_{AGS-FGS}$	Z-score	P-value	FDR	Overlap, N
ECGI10	68	12107	KEGG#00670	18	6178	52	26.08	7.38	3.90E-08	5.50E-07	0
MPP89	24	2268	KEGG#00670	18	6178	19	4.89	8.09	1.70E-10	4.30E-10	1
A2780	127	5823	KEGG#00670	18	6178	10	12.54	-0.77	0.47	1	0
RS411	116	9253	KEGG#00670	18	6178	15	19.93	-0.69	0.27	1	0

243

244

## 245 **2. Construction of sample-specific AGS**

246 In order to analyze data from the *in vitro* cancer cell screens and the primary tumor samples (TCGA) in the  
247 same manner, we constructed AGSs by following the same platform-specific approaches. Intuitively, having  
248 an AGS that is too big or too small could deteriorate specificity or sensitivity of NEA. Therefore, in order to  
249 prove that observed differences are not due to selecting AGS genes in a specific way, we tested and  
250 compared a number of options for AGS compilation. Mutation-based AGSs were created by first listing all  
251 point-mutated genes in each given sample (which might include hundreds and even thousands of passenger  
252 mutations) and then retaining only those with significant network enrichment against the rest of the set. This  
253 approach (Merid, Goranskaya, & Alexeyenko, 2014) had been proposed for distinguishing between driver  
254 and passenger mutations - hence the filtering should reduce noise by enriching AGSs in driver genes. Next,  
255 AGSs from gene copy number and expression data included genes most deviating from the cohort means.  
256 This was achieved by using one of the three alternative algorithms (see Methods). Again, even such deviant  
257 gene sets could still be too large, e.g. due to listing copy number-alterations over extended chromosomal  
258 regions. In order to compact these, alternative AGS versions were derived by retaining only genes with  
259 significant network enrichment for signaling and cancer pathways or for the mutation-based AGS of the same  
260 sample, which reduced the AGS lists 3-10 fold. An alternative to using gene copy number data would be to  
261 account for respective mRNA expression levels. While this approach is subject of ongoing discussion, we  
262 have observed (Merid et al., 2014) that many known copy number drivers did not exhibit this correlation and  
263 therefore we decided not to filter copy number data by the gene expression feature. Finally and as an extra  
264 option, we merged platform-specific AGSs into combined AGSs.

## 265 **3. Statistical power to detect correlates of drug sensitivity**

266 The goal of this first, exploratory analysis was to compare the different methods and feature classes in their  
267 ability to explain the differential drug sensitivity. To this end, we counted features significantly associated with  
268 a phenotype after adjusting the respective p-values for multiple testing. This approach is essentially  
269 equivalent to the Q-Q plot analysis (Wilk & Gnanadesikan, 1968) but enables more quantitative estimation.  
270 For example (Suppl. Fig. 1), we analyzed associations between, on the one hand, all point mutation profiles  
271 of cancer cell lines (Forbes et al., 2014) and, on the other hand, cell lines' sensitivity to each of the 203 anti-  
272 cancer drugs from Basu et al. (Basu et al., 2013). The fraction of low p-values (e.g.  $p(H_0) < 0.001$ ) in the total  
273 number of statistical tests did not exceed that expected by chance (the null hypothesis  $H_0$  was defined as  
274 absence of association between presence of mutation in a gene and the cell line's sensitivity to the drug).

275 Consecutively, no genes received q-values (adjusted p-values) (Storey & Tibshirani, 2003) below 0.05. On  
276 the contrary, the correlation analysis of gene expression data (Barretina et al., 2012) against the same drug  
277 sensitivity profiles discovered nearly 15,000 patterns of association between gene expression and drug  
278 sensitivity (out of in total  $18,900 \times 203 = 3,836,700$  tests) with  $p(H_0) < 0.001$ . After the adjustment, more than  
279 2500 of these gene-drug pairs remained significant at  $q < 0.001$ . These two examples demonstrate how  
280 dramatically the information content could vary depending on the feature type and data origin.

281 Applying this approach to the *in vitro* drug screen data, we compared features of different types and classes  
282 by the amount of information on drug sensitivity they contain. Respectively, in TCGA data we measured  
283 correlations of features with survival of patients who received one of the 42 frequently used drugs in one of  
284 the eight cohorts. We systematically compared different feature types, i.e. original data from high-throughput  
285 platforms and NEA scores as well as classes within the types (e.g. transcriptomics data from Affymetrix vs.  
286 Agilent vs. RNA sequencing). We also analyzed the relative performance of different AGS classes.

287 Overall, the NEA scores at both pathway level (PWNEA) and individual gene node level (GNEA) contained  
288 either the same or larger amounts of information on drug sensitivity compared to the original gene profiles  
289 (Fig. 3). In the drug screen data analysis, the ORA, PWNEA, and GNEA features performed apparently  
290 better than the respective original point mutation, gene copy number, and gene expression data. In the  
291 TCGA data analysis, the advantage of PWNEA and GNEA over both ORA and original gene profiles for  
292 particular drugs was even more pronounced, although not always overall significant. Among the platforms for  
293 the *in vitro* screens, Affymetrix data by far outperformed mutation data, copy number, and combined AGSs.

294 In TCGA datasets, RNA sequencing performed better than Affymetrix (although the former data was not  
295 available for the cell lines). In general, transcriptomics based datasets much more frequently manifested  
296 correlations with drug sensitivity than those based on gene mutations and copy number data (Suppl. Fig. 3).

297 While this observation is not new (Iorio et al., 2016), the most obvious explanation should be that  
298 most of the genome alterations were insufficiently frequent for the statistical tests. As an example, less than  
299 10% of the genes in the BRCA cohort had point mutations in more than 1% of the tumors. On the contrary,  
300 continuous mRNA expression profiles were available for most of the genes in every dataset. At this stage of  
301 the analysis, we also assessed relative performance of the different AGS classes. From each dataset with  
302 continuous values we created AGSs of fixed size (`top.200` and `top.400`) as well as sets of variable size  
303 where genes were included based on significance as referred to the cohort mean (`significant`) and, in  
304 addition to the latter, tested for network enrichment toward cancer gene sets  
305 (`significant.filtered.mini`) or any signaling pathways (`significant.filtered.maxi`). As

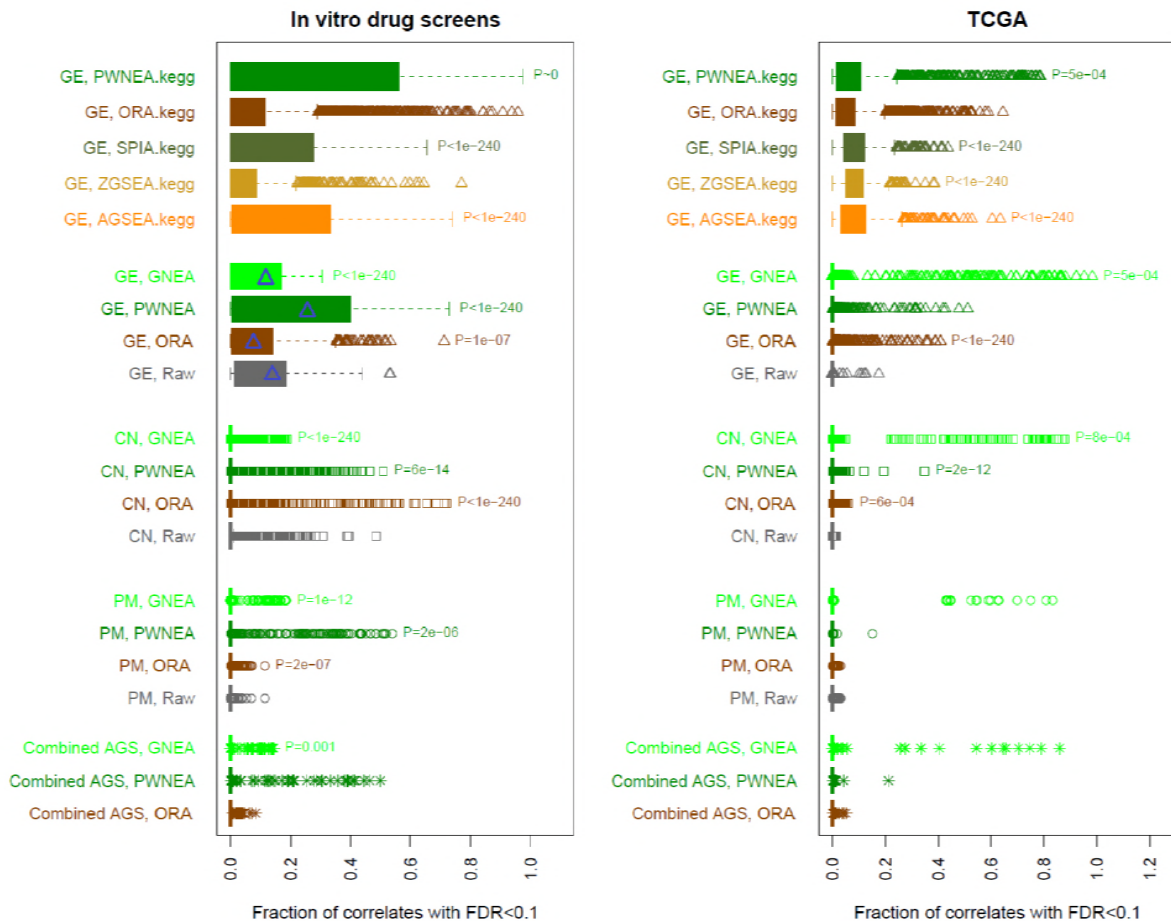
306 illustrated in Supplementary Figure 3, the different classes yielded variable results. We evaluated  
307 consistency and significance of these differences using the same Kolmogorov-Smirnov test as in Figure 3 on  
308 the gene copy number and expression datasets for cell lines and TCGA samples (Suppl. Table 1). This  
309 evaluation, however, did not lead to an unequivocal conclusion. In the cell line datasets, the fixed size AGSs  
310 performed significantly better, while in the TCGA datasets the situation was rather opposite.

311 Figure 3. Comparison of the potential performance of different features, methods, and data types.

312 The top 5 boxplot rows (labeled with “kegg”) present results obtained using the limited set of 197 KEGG pathways (for the  
313 sake of compatibility with SPIA method, which required within-pathway topology information in KGML format) and by using  
314 only gene expression data (label “GE” - for compatibility with SPIA, AGSEA, and ZGSEA). The other boxplot rows present  
315 tests on the full set of 328 FGS, since ORA, PWNEA, and GNEA did not require intra-pathway topology and could accept  
316 any data type. Note that the KEGG pathway versions in the 197 KGML files contained somewhat different gene sets  
317 compared to the KEGG download used in the core set, so the respective PWNEA and ORA values might differ.

318 Each boxplot element combines values of correlation between either original or AGS features for a given class (labeled at  
319 the vertical axis) and for either the *in vitro* response to drugs in the three screens (left pane; in total 365 tests of 320 distinct  
320 drugs) or for the survival of patients who had been treated with drugs (right pane; 42 drugs in the eight TCGA cohorts). As  
321 an example, we calculated Spearman rank correlations between sensitivity of cell lines to drug RITA and transcriptomics  
322 features of these cell lines: either original Affymetrix (CCLE) gene expression profiles (18900 genes) or enrichment profiles  
323 of cell line specific AGSs of class `top.400.affymetirx_ccle` produced by GSEA (328 FGS features), pathway-level  
324 NEA (PWNEA; the same 328 features), and gene-level NEA (GNEA, in which 19027 nodes in the global network were  
325 treated as single-gene FGSs). The p-values of Spearman correlations between features and the drug sensitivity were then  
326 adjusted for multiple testing. The fractions of adjusted p-values below 0.1 became X-coordinates for the plot. The four  
327 examples (indicated by the blue markers), respectively, gave fractions  $1837/18900=0.097$ ;  $23/328=0.070$ ;  $78/328=0.236$ ;  
328 and  $2090/19027=0.110$ . Each boxplot element combined such fraction values for each drug from each screen or TCGA  
329 cohort as well as all alternative AGSs classes for ORA, PWNEA, and GNEA. The features are grouped by type of profiling  
330 (original data, ORA, PWNEA, and GNEA as grey, brown, dark green and bright green, respectively) and by data type (point  
331 mutations, PM; copy number alterations, CN; and gene expression, GE). If a category produced significantly more and  
332 higher non-zero patterns (i.e. fractions with  $FDR < 0.1$ ) than its respective reference, then the p-value for Kolmogorov-  
333 Smirnov test is shown, comparing distributions of this category to that of the reference. The reference for PM, CN, and GE  
334 types were the respective original data. The reference for type 'combined' were ORA categories (since 'combined' AGSs  
335 were created as unions of respective PM, CN, and GE AGSs rather than from original data directly).

336 The boxes contain data points within 25-75th percentile intervals (i.e. between quartiles Q1 and Q3). The maximal whisker  
337 length, MWL, is defined as 1.5 times the Q1-Q3 interquartile range (i.e. the box length). Whiskers can extend to either the  
338 MWL or the maximal available data point when the latter is below MWL. Markers thus correspond to data points that  
339 extend off the box by more than the MWL value.



340

341 While the original features manifested considerable correlations in a number of classes, fractions of  
 342 significant correlations were largely inferior when compared to NEA classes. In general, the different  
 343 methods could be ranked by potential sensitivity in the following order: original gene profiles < [either ORA or  
 344 ZGSEA] < [either AGSEA or SPIA] < [either PWNEA or GNEA]. However even upon adjustment for multiple  
 345 testing, we did not draw ultimate conclusions from significance of these correlations. This exploratory  
 346 analysis only informed us on the relative Type II error rates (i.e. sensitivity, or statistical power to detect  
 347 correlation), suggesting that multiple alternative methods and data types were potentially predictive of drug  
 348 sensitivity. In order to evaluate robustness of these predictions we proceeded to the validation step as  
 349 described below. We also note that only ORA, PWNEA, and GNEA could provide means for integrating  
 350 omics data from different platform (by simple merging of AGS lists), where ORA was apparently inferior.

351

#### 352 4. Consistency of the discovered correlates in different drug screens

353 In order to test reproducibility of the drug-feature associations in alternative experimental settings, we used  
354 data from three *in vitro* drug screens: CCLE (Barretina et al., 2012), CGP (Garnett et al., 2012), and CTD  
355 (Basu et al., 2013). A comparison between CCLE and CGP screens was earlier presented in (Haibe-  
356 Kains et al., 2013). The CTD drug screen was published later and provided additional shared compounds for  
357 our cross-screen analysis (31 in addition to the 16 available to Haibe-Kains and colleagues). Similarly to  
358 these authors, we found that the association values between drug sensitivity and original features only  
359 weakly agreed between the drug screens.

360 Albeit weak, these correlates were still significantly concordant across screens. Fig. 4A presents examples of  
361 between-screen rank correlations when using original gene expression profiles, ORA, PWNEA, and GNEA  
362 features. When comparing results from screens by CGP (Garnett et al., 2012) and CTD (Basu et  
363 al., 2013), the correlation values between Affymetrix expression data and sensitivity to navitoclax ranged  
364 from R=0.31 (original gene profiles) to R=0.81 (GNEA). More systematic analyses demonstrated (Fig. 4, B  
365 and C) that using AGS features in PWNEA and GNEA considerably strengthened the concordance compared  
366 to the original gene profiles and AGSs in ORA. For example, by requiring across-screen rank correlations  
367 above 0.6, four NEA feature classes based on gene copy number performed better than any original copy  
368 number class. Under the same rank correlation threshold, eight out of ten transcriptomics NEA classes and  
369 all those based on point mutations were superior to the respective original data classes. The analysis of  
370 correlation p-values instead of the correlation coefficients yielded similar results (Suppl. Fig. 3). Results  
371 obtained with ORA were, again, inferior to those from NEA and the summarized ranking appeared as:  
372 [original gene profiles and GSEA] < PWNEA < GNEA. In the tests using 197 KGML-KEGG pathways and  
373 gene expression data, SPIA and AGSEA were somewhat superior over PWNEA.

374 Figure 4. Consistency of drug-feature associations between drug screens.

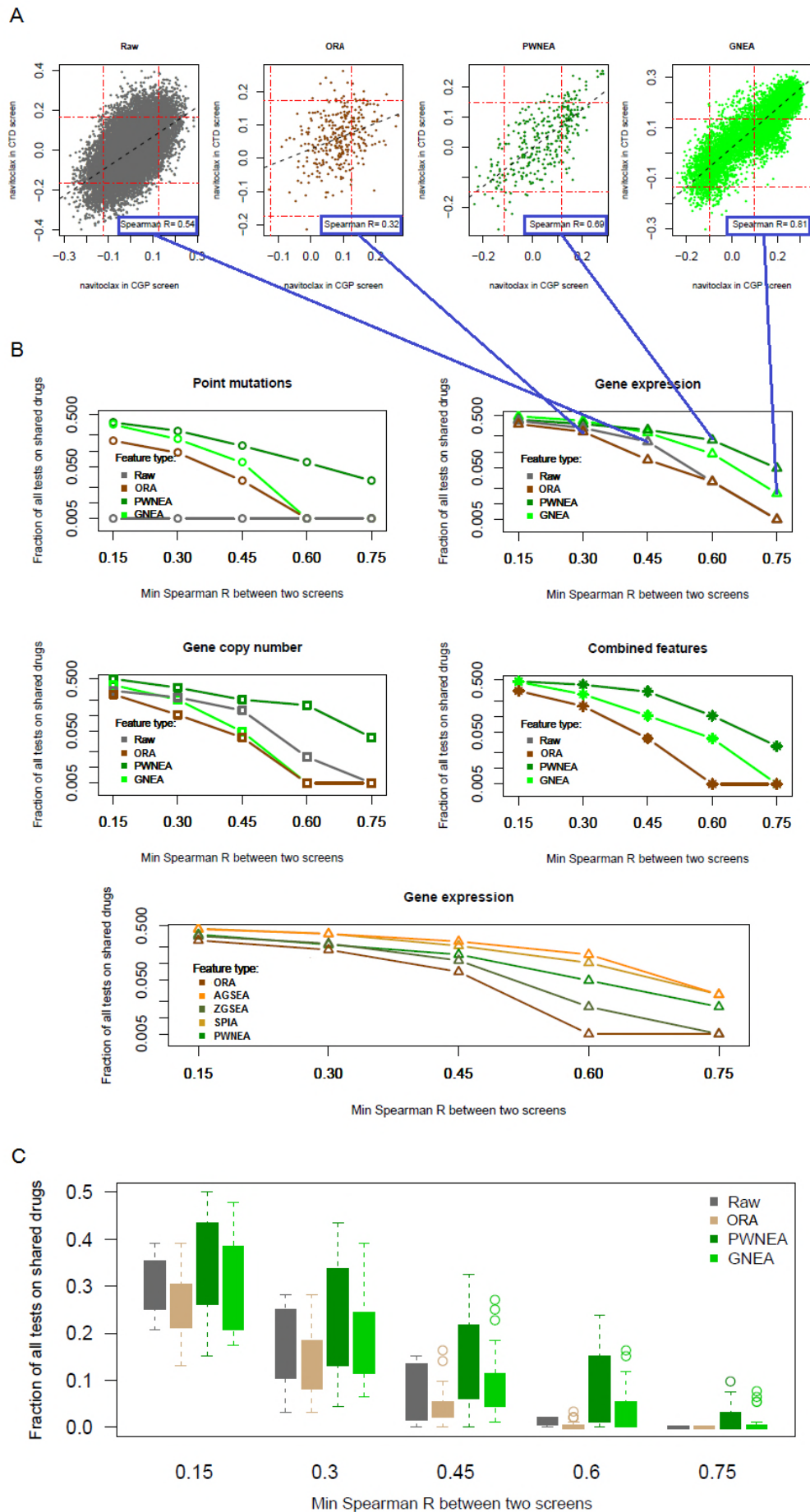
375 For each drug shared by any two of the three *in vitro* drug screens (in total 47 cases), we calculated rank correlation  
376 between drug-feature rank correlation coefficients in the two screens.

377 A. Agreement of drug-feature rank correlation coefficients between CGP and CTD screens of sensitivity to navitoclax  
378 using Affymetrix data as original gene expression values Affymetrix\_CCLE (left pane) and AGS features of class  
379 `significant.affymetrix_ccle` profiled with ORA, PWNEA, and GNEA (other panes). The agreement in this case  
380 was worst upon using ORA profiles (rank R=0.32), whereas GNEA profiles performed best (rank R=0.81). The red lines  
381 indicate the levels of false discovery rate (the correlation p-value adjusted by Benjamini-Hochberg) FDR=0.1. The grey  
382 diagonal line is the linear regression fit.



383 B. Fractions of cases with rank correlation value above each of the five specified thresholds on example AGS classes. The  
384 features are grouped by type of profiling and by data type identically to Fig. 3. In order to characterize sensitivity to each of  
385 the 47 shared drugs, we used here, in parallel with respective original gene profiles, AGS features of one class of each  
386 type: `significant.filtered.exome.mini (PM)`, `significant.filtered.snp6.mini (CN)`, and  
387 `significant.affymetrix_ccle (GE)`, and `significant.filtered.combined.maxi ('combined')` . The  
388 advantage of PWNEA and GNEA became apparent at the two highest cutoffs  $R>0.60$  and  $R>0.75$ . Four example values  
389 from A are mapped to the gene expression plot in B.

390 C. Similarly to B, fractions of values above each of the five specified thresholds were calculated for *all* classes and  
391 combined for all data types. For certain AGS classes, PWNEA and GNEA produced correlates highly conserved across  
392 screens ( $R>0.6$ ) in as many as 5-10% of cases. As an alternative, Supplementary Figure 3 shows an across-screen  
393 comparison of p-values rather than of the raw rank correlation coefficients.



395  
396 We validated drug sensitivity profiles of four anti-cancer compounds, tested previously in the CTD screen -  
397 RITA, PRIMA-1<sup>MET</sup>/Apr-246, nutlin and JQ1 - in a new *in vitro* screen, named ACT. The activities of these  
398 compounds were re-tested in a panel of 20 cancer cell lines (the ACT set) for which the CCLE gene  
399 expression and point mutation profiles data were available. The wide response ranges indicated sufficient  
400 differential response across the ACT set. Similarly to the results in Fig. 3, there were both original gene  
401 profiles and NEA features showing significant, moderately strong correlation with drug sensitivity, which  
402 demonstrated the potential of multivariate models for drug sensitivity prediction.

403 As shown above, the original gene profiles were poorly preserved across drug screens. Therefore, we  
404 compared the CTD results with those from ACT screen in a more relevant multivariate approach using the  
405 "elastic net" method (Friedman, Hastie, & Tibshirani, 2010). Starting from all available features,  
406 each model was finally reduced to a much smaller subset. Multi-variate models are notoriously prone to over-  
407 fitting when the number of variables exceeds the number of samples. For this reason, validation on  
408 independent sets has become an essential requirement in such studies (Committee on the Review of  
409 Omics-Based Tests for Predicting Patient Outcomes in Clinical Trials, Board on  
410 Health Care Services, Board on Health Sciences Policy, & Institute of Medicine,  
411 2012). We thus created CTD-based models using cell lines not found in the ACT screen. The comparison  
412 was also streamlined by using only the data from CCLE Affymetrix and point mutation datasets versus two  
413 respective feature AGS classes `mutations.mgs` and `significant.affymetrix_ccle`. Using other  
414 classes produced similar results (data not shown).

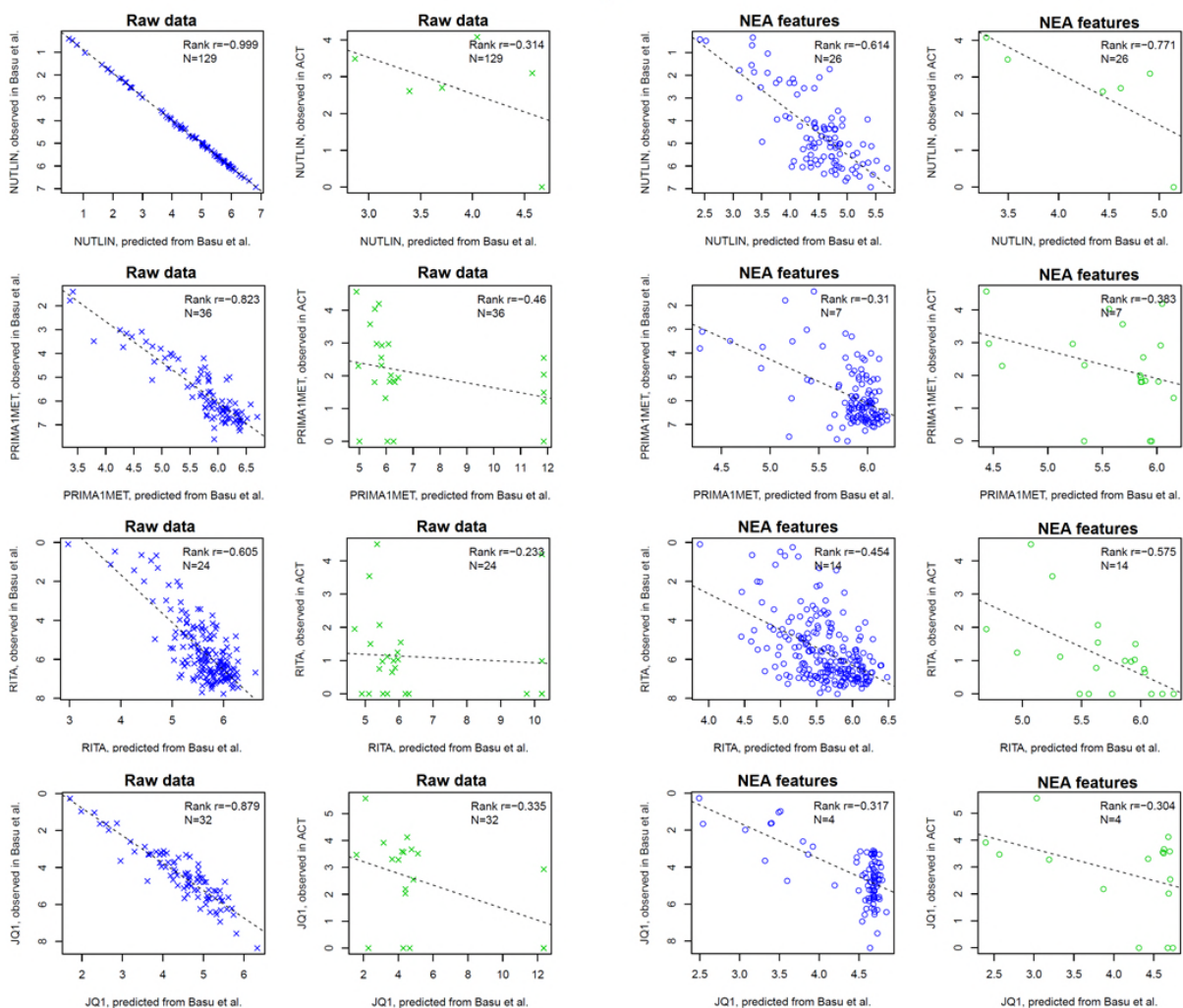
415 Figure 5 demonstrates that by applying common elastic net parameters, in every case it was possible to  
416 obtain a descriptive model from CTD drug screen data with a number (4...129) of non-zero terms and then  
417 substantiate the model (possibly with a poorer performance) using the ACT data in a smaller cell line set. For  
418 each modeled case, we compared observed and predicted drug sensitivity values. The most important  
419 observation was that in all instances without exception the signs of these correlations were consistent  
420 between CTD model and ACT validation, i.e. negative correlations in the training set remained negative upon  
421 validation.

422

423 Figure 5. Predicted versus observed drug sensitivity across cancer cell lines in discovery versus validation  
424 screens.

425 The predictive models for four compounds tested in the published CTD screen were validated in our ACT screen.  
426 Elastic net models were built under cross-validation (columns 1 and 3, blue) and then tested on non-overlapping sets  
427 of cell lines of the ACT screen (columns 2 and 4, green). Input variables were either original gene point mutation and  
428 expression profiles (columns 1 and 2, crosses) or PWNEA scores derived from these datasets for each cell line  
429 (columns 3 and 4, circles).

430 Legends in each plot display the values of Spearman rank correlation between observed and predicted values ('Rank  
431 r') and the number of non-zero terms in the model ('N'). Parameter alpha for the shown plots was set to 0.9. Since  
432 the drug sensitivity values from CTD screen were inverted compared to the other screens, the correlations are  
433 presented as negative values (see also inverted vertical scales for "observed in Basu et al."). Detailed plots for  
434 models built under different alpha parameters are found in Supplementary Files  
435 glmnetModels.Basu\_vs\_new.raw.pdf and glmnetModels.Basu\_vs\_new.pwnea.pdf.



436

437

438 Overall, the performance of the original profile models on the validation sets appeared comparable to that of  
439 PWNEA. However importantly, the former had much more freedom in model term selection since the initial  
440 feature space was around two orders of magnitude larger than that in PWNEA. Consequently, despite the  
441 rigorous cross-validation and feature selection implemented in the `glmnet` algorithm, using the original  
442 profiles generated more complex models (see the number of terms per model,  $N$ ) which fit the training sets  
443 better (and were close to overfitting in the case of `nutlin`). At the validation step however, the performance of  
444 the original data based models significantly worsened - whereas the performance of PWNEA-based models  
445 remained at roughly the same level (all results obtained under variable parameters can be found in  
446 Supplementary Files `glmnetModels.Basu_vs_new.raw.pdf` and `glmnetModels.Basu_vs_new.pwnea.pdf`).  
447 Therefore, this result essentially corroborated the previous conclusion about lower robustness of the original  
448 gene profiles compared to NEA.

#### 449 **5. Agreement between *in vitro* screens and clinical data**

450 A much more challenging task was to identify a conservation of associated features between the *in vitro* drug  
451 screens and clinical application of the same drugs. Any trustworthy setup of such an analysis would be very  
452 complex, so that even cross-validation and adjustment for multiple testing could not guarantee unbiased  
453 probabilistic estimation, such as true discovery rate. Thus, the final judgment should be made after a  
454 biologically independent *ad hoc* validation from the *in vitro* to the clinical domain. The TCGA data collection  
455 would not allow creating correctly balanced, randomized cohort designs for estimation of relative risks, error  
456 rates etc. However, our task was simplified by only needing to compare the methods' performance. A  
457 somewhat skewed cohort composition was unlikely to cause differences in robustness between e.g. original  
458 gene expression profiles and corresponding NEA scores.

459 In the eight largest TCGA cohorts, we counted how many significant *in vitro*-detected features correlated  
460 with survival of patients who received same drug (Cancer Genome Atlas Research Network, 2008),  
461 (<https://tcga-data.nci.nih.gov/docs/publications/tcga/>; Suppl. Table 4). More specifically,  
462 molecular features of each class (such as point mutations, gene expression profiles, or AGS enrichment  
463 profiles) that were significantly correlated with sensitivity to a drug in cell lines were required to be also  
464 significantly correlated with patient survival in a TCGA cohort. Beyond the drug administration data and the  
465 features, our survival analysis accounted for clinical covariates available from TCGA (Suppl. Table 4). The  
466 latter enabled estimating the 'net' effects of molecular features, i.e. what they convey beyond the known  
467 clinical information, such as e.g. ER status in the breast cancer.

468 We matched correlates of same data types in CCLE and TCGA (although possibly obtained using different  
469 omics platforms, e.g. Affymetrix microarray could be matched to RNA-seq etc.). Then we determined  
470 whether correlation p-values of individual features, in their turn, correlated between *in vitro* and TCGA data,  
471 i.e. if genes or FGSs with high (respectively low) correlation with drug response *in vitro* tended to correlate in  
472 the same manner with the patients' response. Due to the testing of alternative AGS classes, respective  
473 numbers of matching pairs in ORA, PWNEA, or GNEA were an order of magnitude higher than in raw data  
474 (column 2 in Table 3). Therefore we coupled this calculation with a significance test by randomly permuting  
475 feature and sample labels. Altogether, the permutation tests indicated that point mutation and copy number  
476 data had zero true discovery rates (TDR), i.e. their correlation p-values were preserved not more often than  
477 expected by chance (see column 3 in Table 3). On the contrary, the TDR levels were substantial  
478 (0.033...0.805) for gene expression data and for AGSs processed with each of the three enrichment  
479 analyses ORA, PWNEA, and GNEA.

480 At the next step (remaining columns of Table 3) we calculated the numbers of significant cases that would  
481 also be practically usable, i.e. had both lower p-values (<0.001) and rank correlation values higher than 0.2.  
482 No such cases were identified in the gene expression data. ORA, PWNEA, and GNEA yielded 0.8%, 3.5%,  
483 and 5.9% of practically usable cases, respectively. Interestingly, most (56 out of 78) of the ORA cases were  
484 identified in the breast cancer cohort, whereas the preserved PWNEA and GNEA correlations distributed  
485 uniformly across all the TCGA cohorts, except prostate cancer which cohort shared only one drug with one *in*  
486 *vitro* screen. Remarkably, the separate test using the 197 KGML KEGG pathways also demonstrated  
487 superiority of PWNEA over ORA, ZGSEA, AGSEA, and SPIA - despite the competitive performance of the  
488 latter two in the previous sections. Thus at this crucial stage of our analysis, robustness of the data types  
489 while translating drug sensitivity correlates between *in vitro* and clinical applications increased in the  
490 following order: [point mutations and gene copy number changes] < [gene expression] < [ORA, ZGSEA,  
491 AGSEA, and SPIA] < PWNEA < GNEA.

492

493 Table 3. Conservation of drug sensitivity correlates between the *in vitro* drug screens and clinical  
494 applications.

Feature type		No. of available "feature X drug" tests	True discovery rate by permutation test, $p(H_0) < 0.01$	No. of usable correlates, so that $p(H_0) < 0.001$ and rank $R > 0.2$								
				All TCGA cohorts (% of available correlates)	Bladder carcinoma, BLCA	Breast carcinoma, BRCA	Colon adenocarcinoma, COAD	Glioblastoma multiforme, GBM	Lung adenocarcinoma, LUAD	Lung squamous carcinoma, LUSC	Ovarian carcinoma, OV	Prostate adenocarcinoma, PRAD
Original gene profiles	Point mutations, PM	360	0	0	0	0	0	0	0	0	0	0
	Copy number alterations, CN	522	0	0	0	0	0	0	0	0	0	0
	Gene expression, GE	1080	0.149	0	0	0	0	0	0	0	0	0
Enrichment analysis	ORA	9014	0.033	78 (0.8%)	0	56	0	3	3	8	8	0
	PWNEA	8822	0.146	305 (3.5%)	18	60	20	52	51	45	59	0
	GNEA	8630	0.805	505 (5.9%)	15	84	46	113	93	72	82	0
Enrichment analysis, GE on KEGG only	ORA	5252	0.025	21 (0.3%)	0	5	0	2	4	2	8	0
	ZGSEA	1080	0.037	8 (0.7%)	0	2	0	0	1	0	5	0
	AGSEA	1080	0.02	7 (0.6%)	0	7	0	0	0	0	0	0
	SPIA	1080	0.048	3 (0.3%)	0	0	0	3	0	0	0	0
	PWNEA	4988	0.241	364 (7.2%)	44	83	20	79	27	19	92	0

495  
496

497 The purpose of the analysis above was to prove systematic significance of the produced correlates. We  
498 reiterate that using the original data did not seem efficient: although many transcriptomics profiles correlated  
499 with drug sensitivity, those patterns could not be traced back to the *in vitro* screens.

500 Most of the consistent NEA features were obtained for AGS based on gene expression data (Suppl. Table 2).  
501 They were identified for docetaxel, gemcitabine, and paclitaxel in BRCA (see the cancer cohort notation in  
502 Table 3); for dexamethasone, erlotinib, and topotecan in GBM; for gemcitabine in LUAD; and for

503 gemcitabine, paclitaxel, tamoxifen, and topotecan in OV. While using gene copy number data, consistent  
504 PWNEA and GNEA features were found only for GBM (dexamethasone and topotecan). Consistent features  
505 that correlated with the response to cisplatin (LUSC) belonged to the combined, multi-platform types. Only  
506 one consistent GNEA feature was based on somatic mutation analysis (gemcitabine in LUSC), although it did  
507 not match all of the criteria. Below we present promising features found in the drug screens, which were also  
508 predictive of survival if the drug was administered in a TCGA cohort.

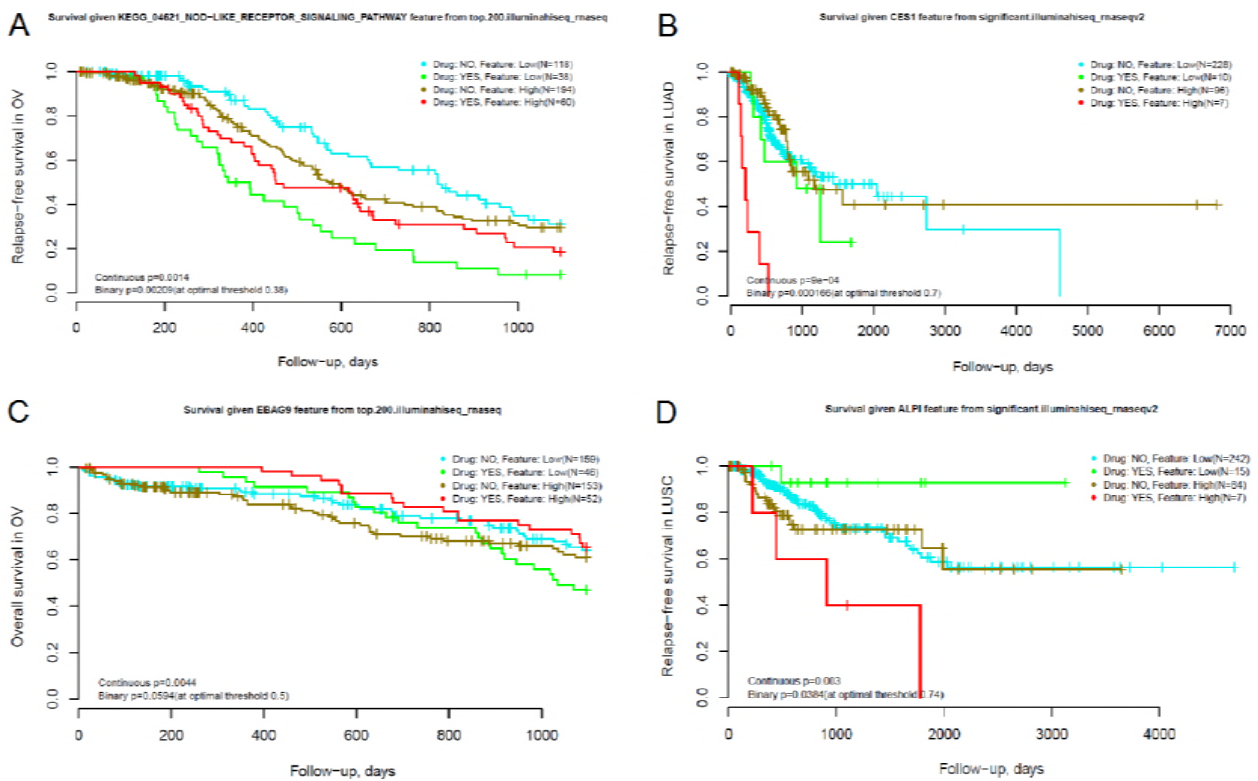
509 The cancer emergence and progression were earlier linked to tissue inflammation through the NOD-like  
510 receptor signaling (Saxena & Yeretssian, 2014) . We found that the corresponding pathway score correlated  
511 with survival in ovarian carcinoma patients treated with topotecan (Fig. 6A).

512



513 Figure 6. Clinical performance of NEA features discovered in drug screens.

514 Each TCGA cohort was split into four categories by two factors: 1) administration of the specific drug and 2) predictive  
515 feature value (pathway or individual gene score, indicated in the plot header), each above and below a threshold. The  
516 primary feature evaluation employed p-values calculated in the continuous score space, i.e. without splitting the  
517 patient cohort into binary classes by factor (2) and then the binary classifications by the both factors were used for  
518 visualization (as “treated/untreated” for the drug and at the quantile “optimal threshold” value for the quantitative NEA  
519 feature). The p-values are shown for the both alternatives. The plots present differential survival upon treatment with  
520 topotecan in ovarian carcinoma (A and C), gemcitabine in lung adenocarcinoma (B), and vinorelbine in lung  
521 squamous cell carcinoma (D).



522

523

524

525 Carboxylesterases (CESs) are capable of hydrolyzing gemcitabine (Williams et al., 2011) - for  
526 instance, CES2 is capable of slowing down hydrolysis of the gemcitabine pro-drug LY2334737 (Pratt et  
527 al., 2013). We identified as many as 31 gene-wise NEA features which correlated with relapse-free  
528 survival in lung adenocarcinomas treated with gemcitabine. This list of network nodes from the GNEA  
529 included CES1 (Fig. 6B), CES2, CES7, and a number of cytochromes with possible involvement in the  
530 catabolism of xenobiotics. Many of these genes were AGS members in both the gemcitabine-sensitive cell  
531 lines and in patients who responded to the gemcitabine treatment and – at the same time - they themselves  
532 were members of KEGG pathways 00980 “Metabolism of xenobiotics by cytochrome p450”, 00983 “Drug  
533 metabolism – other enzymes, and 00982 “Drug metabolism – cytochrome p450”. Consequently, the ORA  
534 and PWNEA analyses detected enrichment of these pathways in the same patients. However the pathway  
535 scores correlated with response to gemcitabine neither in the CCLE and CTD screens nor in the LUAD  
536 cohort) and therefore would be useless as biomarkers. The gene expression profiles of carboxylesterases  
537 and cytochromes in cell lines and primary tumors did not correlate with gemcitabine response either. EBAG9  
538 had been implicated previously in ovarian cancer progression (Akahira et al., 2004), but it has not  
539 been shown to affect response to topotecan. Indeed, in the datasets of our study the expression of the gene  
540 itself correlated neither with cell line sensitivity to topotecan nor with patient survival. However, the GNEA  
541 features for EBAG9 as a network node did correlate with sensitivity to topotecan *in vitro*  
542 (`top.200.affymetrix_ccle`;  $p(H_0)=4.2\times 10^{-11}$ ) and with overall survival of OV patients (Fig. 6C)  
543 (`top.200.illumina_hiseq_rnaseq`;  
544  $p(H_0)=4.4\times 10^{-4}$  during the 3-year follow-up time while accounting for "clinical stage" as a covariate).  
545 The intestinal-type alkaline phosphatase ALPI is known to be a modulator of cancer cell differentiation (Shin  
546 et al., 2014) and cytoprotection (Giatromanolaki, Sivridis, Maltezos, & Koukourakis,  
547 2002), (Ritz, Baty, Streibig, & Gerhard, 2015). In our analysis its GNEA feature was, in  
548 parallel with eleven others, negatively correlated with sensitivity to vinorelbine *in vitro*  
549 (`gnea.significant.affymetrix1`;  $p(H_0)=1.1\times 10^{-07}$ ) and with overall survival of OV patients  
550 ( $p(H_0)=0.003$ ; Fig. 6D).  
551 This setup could not eliminate possible confounding effects from multi-drug treatment history and clinical  
552 factors that might determine administration of specific drugs. Nonetheless, the NEA scores apparently  
553 explained the differential sensitivity to anti-cancer drugs in a much more robust and efficient manner than the  
554 original data.

555 Apparently, multiple false positives would be generated by accepting raw p-values of the “drug X feature”  
556 interaction terms without adjustment (0.0014, 0.0009, 0.0044, 0.0030 in Fig. 6A...D, respectively). For  
557 instance, 57 errors of Type I could have been made at  $p=0.003$  while evaluating the 19027 GNEA features. A  
558 commonly accepted ‘omics’ adjustment (Storey & Tibshirani, 2003) is poorly suited for multifactorial  
559 models where p-values are statistically coupled within models. However, since these examples were  
560 selected from cell line screen correlates, we can combine them by using Fisher’s method (Robert A.  
561 Fisher, 1925) with respective p-values (2.23e-09, 2.20e-07, 4.18e-11, 8.15e-08). This yielded combined  
562 p-values as low as 8.58e-11, 4.62e-09, 5.58e-12, and 5.65e-09, respectively. At this level, the numbers of  
563 expected false discoveries approached zero.

564 A visual inspection of the survival curves in Fig. 6 sheds light on usefulness of these tentative biomarkers in  
565 a clinical setting. As an example, in a 1-year survival perspective, relative risks (RR) would either increase  
566 (Fig. 6A,C) or decrease (Fig. 6B,D) given higher NEA scores of the patient samples. By using this fixed  
567 follow-up interval and the cohorts of limited size, the confidence intervals at the 95% level would be rather  
568 broad:  $\ln(\text{RR}) = 0.405$  (95% CI: [-0.07...0.88]);  $\ln(\text{RR}) = -2.061$  (95% CI: [-3.99...-0.13]);  $\ln(\text{RR}) = 2.211$   
569 (95% CI: [-0.70...5.12]);  $\ln(\text{RR}) = -2.181$  (95% CI: [-5.15...0.78]) for Fig. 6A...D, respectively. The fractions of  
570 patients who might benefit from using these predictors could be estimated in terms of absolute risk reduction  
571 as 0.17, 0.62, 0.08, and 0.25. Inversely, the “number needed to treat”, i.e. how many patients should be  
572 treated for one individual to benefit from the new test would have been 6.00, 1.60, 12.91, and 3.94,  
573 respectively (Laupacis, Sackett, & Roberts, 1988). However, additional responders could be  
574 detected by using other markers, used in parallel. As an example, beyond the “NOD-like receptor signaling  
575 pathway” at Fig. 6A, the response to topotecan in ovarian cancers similarly correlated with KEGG pathways  
576 “One carbon pool by folate” and “Bacterial invasion of epithelial cells” as well as with the GO term “Cytokine  
577 activity” (not shown). Predictions made with these markers would overlap only partially and therefore can  
578 complement each other. We presume that such discoveries should ultimately be evaluated by independent  
579 validation and careful clinical development. In fact, our combined analysis of independent cell screen and  
580 clinical results gave a first example of such validation.

581

## 582 DISCUSSION

583 We have presented a way of using network enrichment scores for prediction of drug response and  
584 demonstrated its advantage compared to the conventional analyses of original gene profiles and alternative  
585 enrichment methods. In comparison to the latter, the NEA scores correlated stronger with drug sensitivity and  
586 were preserved better between independent screens. Multivariate models using NEA scores proved more  
587 compact and, at the same time, robust when re-tested on newly obtained data. Finally, corroborating *in vitro*  
588 phenotypes in corresponding clinical applications was possible by using the NEA scores but not by original  
589 profiles or alternative methods.

590 In our view, the advantages of our approach are due to the following features of network-based data  
591 interpretation: 1) combining major types of molecular interactions in a biologically relevant way, 2)  
592 summarizing seemingly disparate molecular alterations at the level of pathways and processes, and 3)  
593 enabling lower-dimensional statistical analysis. In addition, network views provide better grounds for  
594 biological interpretation and mechanistic studies. The types of evidence behind the edges (such as protein-  
595 protein interactions, mRNA co-expression, sub-cellular co-localization) might contribute to the integrated  
596 network differently. We refer to the previously published comparative analyses of the contributions (Andrey  
597 Alexeyenko & Sonnhammer, 2009), (Merid et al., 2014), (A. Alexeyenko et al., 2012). The poor performance  
598 of the individual gene analysis and ORA could be explained by the excessive dimensionality of the former  
599 and poorer sensitivity of the latter (Fig. 1A). In addition, the ability to use smaller and hence more specific  
600 AGS could have provided extra advantage of NEA over ORA. On the other hand, NEA could deteriorate on  
601 AGS of insufficient size or while using sparser networks (around  $10^4 \dots 10^5$  edges) and networks with many  
602 missing nodes. These potential limitations were established earlier (Merid et al., 2014) and we tried to avoid  
603 them in the present work. Still, certain AGS of e.g. class `significant` could become empty when no single  
604 gene would significantly differ from its cohort mean. Also there could be no edges connecting an AGS to a  
605 specific FGS (even though such cases would still have certain variability of NEA scores due to variable  
606 values of  $\hat{n}_{\text{AGS-FGS}}$ ). We admit that a future, more comprehensive version of NEA might adopt advantages of  
607 the alternative enrichment methods by employing full gene lists (as in GSEA) and intra-pathway topology (as  
608 in SPIA). Indeed, at two steps of our analysis these methods demonstrated performance comparable to that  
609 of NEA (Fig. 3 and 4). Given the present state of the data, we could not test here PARADIGM, the method of  
610 using information from multiple platforms, although it should be also employed at some point in the future.

611 A common problem of method benchmarking is the unavailability of ground truth. In our case, too, we did not  
612 possess a set of truly existing molecular correlates of drug sensitivity. Comparing alternatives by the total  
613 number (fraction) of positives would not enable a proper control of the false positive rate. In similar situations,  
614 when it was impossible to distinguish between true and false positives, authors often chose to present  
615 biologically sensible examples, such as enrichment of a pathway pertinent to the problem (Andrey  
616 Alexeyenko et al., 2012), (Glaab, Baudot, Krasnogor, Schneider, & Valencia, 2012) or correlation with a  
617 known drug target (Crystal et al., 2014). In the present work, we evaluated concordance of phenotype  
618 correlations between different, independently collected datasets. This allowed us to circumvent the problem  
619 of false positives via a more compelling prove: the methods were compared by the fractions of corroborated  
620 findings.

621 We started with analysis of drug screens using samples from The Cancer Cell Line Encyclopedia (Barretina  
622 et al., 2012), which were profiled for somatic point mutations, gene copy number changes, and gene  
623 transcription (Forbes et al., 2014), (Garnett et al., 2012), (Barretina et al., 2012). Consequently, in  
624 TCGA cohorts we focused on the same data types. The individual molecular phenotypes were characterized  
625 with AGSs compiled using a number of alternative methods. The analysis provided a primary comparison of  
626 their relative performance but – at the current stage – did not enable definite conclusions about performance  
627 of the different AGS classes. Indeed, AGS of fixed size (`topN`) versus variable size (`significant`)  
628 compared differently in the cell lines versus the TCGA data (Suppl. Table 1). Further in the analysis of  
629 consistency *in vitro* versus clinical results, these classes were almost equally represented (Suppl. Table 2).  
630 We have also seen differences between different filtering approaches in AGSs of classes  
631 `significant.mini` and `significant.maxi` (Suppl. Fig. 2). Therefore an issue to be investigated  
632 further is the comparative performance and robustness of different feature classes, platforms etc.  
633 Importantly, multiple platforms' data can be integrated into combined AGSs. Although in our analysis such  
634 AGSs did not perform much better than platform-specific ones (most likely due to the domination of  
635 transcriptomics data), a more detailed evaluation should be done, including new platforms from TCGA and  
636 elsewhere, such as DNA methylation, protein phosphorylation etc. Given the diversity of carcinogenesis  
637 routes and the multiplicity of respective molecular mechanisms, combining platforms appears essential and  
638 most promising. Incorporation of approaches from sparse linear regression modeling, SPIA, GSEA, and  
639 PARADIGM certainly represent promising ways in this direction.

640 The statistical power of NEA was obviously far from full. As an example, there were 13 drugs for which the  
641 numbers of tested cell lines and patients treated in TCGA cohorts were sufficient for a significant estimation.  
642 For four drugs out of these 13, no reliable correlates could be found. One instructive example could be  
643 irinotecan, prescribed to 25 and 22 patients in COAD and GBM cohorts, respectively. The interesting feature  
644 of irinotecan is that its pharmacokinetic pathway involves the same enzymes as that of gemcitabine (Fig.  
645 6B), namely CES1, CES2, CYP3A4, CYP3A5 and some others  
646 ([https://en.wikipedia.org/wiki/Irinotecan#Interactive\\_pathway\\_map](https://en.wikipedia.org/wiki/Irinotecan#Interactive_pathway_map)) – although the enzymes here work in an  
647 opposite direction: they activate irinotecan rather than degrade as they do with gemcitabine. Nonetheless,  
648 relevant GNEA scores might have been informative for response to irinotecan. The patients' response was  
649 sufficiently differential, too: while all the irinotecan-treated patients relapsed, the time to relapse varied from  
650 78 to 1265 days. However, we did not observe almost any sensible correlation of the pathway genes neither  
651 as GNEA features nor as raw gene expression profiles. In case of GNEA, this suggested that the AGSs of  
652 respective responders (or non-responders) did not have enough network linkage to the irinotecan pathway.

653 Further, our FGSs were created by third-party sources and never meant to be used in NEA. Thus, another  
654 step for NEA-based biomarker discovery would be the compilation of novel, specifically optimized FGSs.  
655 Ultimately, one could compile *de novo* pathways - similarly to the approach by Alcaraz et al., 2017 -  
656 but specifically informative of the drug response or disease prognosis. An example of such a functional set  
657 could be the presented above combination of the ten carboxylesterases and cytochromes.

658 Finally, given the low overlap of member genes between individual AGS, it is important to establish how  
659 AGS-level biomarker panels would practically summarize gene-level information and organize the  
660 accompanying statistical framework. Ways to compile and employ multi-platform AGSs, optimal FGS design,  
661 and construction of NEA-based biomarker panels should therefore become the topics of future studies.

662

## 663 MATERIALS AND METHODS

### 664 *Drug screens*

#### 665 Cell lines used in ACT screen

666 In this analysis, we used 20 cancer cell lines for which molecular data could be found in the CCLE Affymetrix  
667 set as well as in both CCLE and COSMIC point mutation sets: A375, HCT116, HDLM2, HT29, JVM2, K562,  
668 L428, MCF7, MDAMB231, MV411, NB4, PL21, RAJI, RKO, SJSA1, SKBR3, SKNAS, SW480, T47D, and  
669 U2OS. Eight of these cell lines had also been included in the CTD screen (A375, HCT116, HT29, MCF7,  
670 PL21, RKO, SW480, and U2OS). In order to avoid overlap in the multivariate models, we excluded these  
671 eight cell lines while training the original models from the CTD data and only used them in the validation set.

#### 672 Assay for cell proliferation used in ACT screen

673 Cell proliferation was estimated with the WST-1 assay (water soluble tetrazolium). Briefly, cells were  
674 incubated with each drug for 72 hours in a 96-well plate. At the end of this period, they were incubated with  
675 WST-1 reagent (Roche) for 2 hours. Absorbance at 450nm was measured following the instructions from the  
676 manufacturer. The cell proliferation rate compared to that in the control was calculated.

677 For adherent cultures, cells were attached overnight before adding the compounds. For hematological  
678 malignancies, the compounds were added simultaneously with seeding cells. The initial cell density was  
679 chosen so as to avoid confluence at the end of the assay. Each compound was applied in six consecutive 3-  
680 fold dilutions. In all cases except JQ1, the stock for each drug was established at the concentration based on  
681 efficacy determined individually for each drug. Final concentrations were for RITA: 0.01, 0.04, 0.12, 0.37,  
682 1.11, 3.33  $\mu\text{M}$ ; for Apr-246/PRIMA-1-met: 0.3, 1, 3, 9, 28, 83  $\mu\text{M}$ ; for Nutlin-3a: 0.14, 0.41, 1.23, 3.7, 11.11,  
683 33.33  $\mu\text{M}$ . For JQ1 the cell lines HDLM2, HT29, MCF7, RAJI, RKO, SJSA1, SKBR3, and SW480 were  
684 tested using the final concentration range 1.66...0.007  $\mu\text{M}$  in 1:3 serial dilutions. However later we found it  
685 necessary to raise the concentration by one order of magnitude, so that the final concentrations for the rest  
686 of the cell lines were 16.66, 5.55, 1.85, 0.61, 0.20  $\mu\text{M}$ . Then we respectively adjusted IC50 values for the first  
687 group as if they were tested under the final concentrations. This was done by incrementing the initial-stock  
688 IC50 values of HDLM2, HT29, RKO, and SW480 by  $\log_3(10) \approx 2.09$ . The cell lines MCF7, RAJI, SJSA1,  
689 SKBR3 did not show any sensitivity while using the initial stock (IC50 = 0), so that their IC50 values upon  
690 JQ1 treatment were declared missing.

691 IC50 was defined as the drug concentration inducing a 50% reduction in cell proliferation compared to the  
692 control. In the quantitative analysis, we used a universal scale for all the four drugs where units 1...6 stood  
693 for dilution steps (1=1:300; 2=1:900; 3=1:2700; 4=1:8100; 5=1:24300 and 6=1:72900). Sensitivity to  
694 compounds was expressed in IC50 values varying from 0 (insensitive to compound) to 6 (fully sensitive to  
695 compound).

696 IC50 values and p-values of the model parameters were calculated using function `drm` from R package `drc`  
697 (Ritz et al., 2015). The model form (argument `fcn`) was chosen as LL.4, where model parameters `Lowest`  
698 and `Highest` were fixed at cell proliferation rates 0% and 100%, respectively, while parameters `slope` and  
699 `IC50` were left unfixed.

700 The IC50 values are provided as Supplementary File IC50values.ACTscreen.xlsx.

#### 701 **CCLC screen**

702 Barretina et al. (Barretina et al., 2012) analyzed cell line sensitivity to 24 drugs in 504 cell lines. These  
703 authors considered a range of numeric sensitivity metrics for their analysis and finally preferred 'normalized  
704 activity areas'. These original units were calculated as areas under compound response curves where higher  
705 values corresponded to higher sensitivity so that 0 stood for 'insensitive to compound' and 8 corresponded to  
706 'full sensitivity'. Further, the activity area values were normalized for unequal luminescence in the assay. We  
707 rendered them normally distributed by log-transformation. Thus the values in our analysis range from -3.00  
708 meaning 'insensitive to compound' to +2.31 meaning 'maximal sensitivity'.

#### 709 **CGP screen**

710 Garnett et al. (2012) (Garnett et al., 2012) analyzed 138 drugs in 714 cell lines. They used a combination of  
711 IC50 and the slope parameter to achieve the most complete description of responses. We decided to use the  
712 AUC as a single feature that reflects the both values. AUC was originally provided in the same table and  
713 ranged from 0% (fully sensitive) to 100% (insensitive). To approach the normal distribution, we transformed  
714 the values as  $\log(1 - \text{AUC})$ , so that now they ranged from -8.11 meaning 'insensitive to compound' to 0  
715 meaning 'maximal sensitivity'.

#### 716 **CTD screen**



717 The authors (Basu et al., 2013) (Basu et al., 2013) mainly used areas under curve (AUC) for their quantitative  
718 analysis of 203 drugs in 242 cell lines. We reproduced this approach in our study. In completely insensitive  
719 cases, the full area under eight experimental points reached 8, whereas 0 stood for full sensitivity. Thus, the  
720 scale of this screen was inverted compared to the other screens, which was considered in all calculations.

## 721 *Molecular data*

### 722 **Gene expression**

723 The profiling was performed in CCLE study using Affymetrix GeneChip® Human Genome U133 Plus 2.0  
724 Array and in CGP study by Affymetrix GeneChip® HT Human Genome U133 Array plate. The expression  
725 datasets were normalized as described by the authors and made public. Expression profiles in the CTD  
726 study were from CCLE. It has been shown earlier (Haibe-Kains et al., 2013) that disagreement between CGP  
727 and CCLE could be attributed to the usage of different transcriptomics datasets only to a minor extent. We  
728 checked both the CCLE and CGP expression profiles and concluded that the latter provided poorer statistical  
729 power in regard to drug sensitivity as well as lower coverage of both genes (13891 unique mapped gene  
730 symbols vs. 18900 in CCLE) and cell lines (622 vs. 1034). For these reasons, we used the CCLE dataset in  
731 all the presented analyses. Expression values  $x$  of the downloaded datasets were transformed to  $\log_2(x)$ .

### 732 **Gene Copy Number**

733 CCLE, CGP, and CTD all employed Affymetrix SNP 6.0 microarrays for gene copy number detection. We  
734 downloaded the CCLE dataset (Barretina et al., 2012) for 994 cell lines. In addition, we downloaded  
735 COSMIC data (Forbes et al., 2014) independently produced by the same platform and then post-processed  
736 in three different ways to provide total, absolute copy number per gene, number of copies of the minor allele,  
737 and a binary classification of gene copy number values into "gain" vs. "loss". All datasets were used as  
738 downloaded, without further processing or normalization.

### 739 **Point mutations**

740 CCLE provided point mutation data on sequencing of 1667 genes in 904 cell lines. In addition, we  
741 downloaded COSMIC data from exome sequencing of 1023 cell line genomes, which mapped to 19759  
742 gene symbols. Mutation data from the both screens were used in the binary form, i.e. all specifying attributes  
743 were neglected.

744 Following the same approach, we employed TCGA data on somatic point mutations reported in MAF files.  
745 The column 'Variant\_Classification' contained a number (more than 15) different codes, most frequent being  
746 Missense\_Mutation, Nonsense\_Mutation, and Silent. Since the latter constituted around 25% of the total  
747 number of somatic mutations reported in the eight cancers - which would not significantly affect the false  
748 positive and true discovery rates - we analyzed records with any such codes as potentially associated with  
749 drug response.

### 750 *Alternative Methods of Pathway and/or Enrichment Analysis*

751 We evaluated a number of existing multivariate, enrichment-based, and/or network analysis methods that  
752 could be potentially useful in the proposed analysis, accounting for their complexity, applicability to different  
753 experimental designs, and the ability to analyze individual samples rather than the whole cohort. Various  
754 statistical algorithms have been proposed to quantify functional relevance of pathways and other gene sets  
755 by accounting for gene network topology.

756 A number of methods can generate sparse regression models via network-based regularization, i.e. account  
757 for topological relations between potential predictors (typically gene expression variables). The regularization  
758 is based on certain assumptions, such as that e.g. term coefficients of neighbor nodes should be zeroes or  
759 non-zeroes simultaneously (S. Kim, Pan, & Shen, 2013), that edge confidence weights should influence  
760 penalties on the model coefficients (Li & Li, 2008), or that there exists equivalence (or at least parallelism)  
761 between connectivity of nodes and covariance of model terms (Zhao & Shojaie, 2016), (Dirmeier, Fuchs,  
762 Mueller, & Theis, 2017). Advanced regularization of linear models in these methods often demonstrated  
763 promising efficiency (Shojaie & Michailidis, 2010). However being very sophisticated, these models proved  
764 hard to tailor to novel, specific experimental designs. Notably, it was not feasible to include additional  
765 covariates or interaction terms which would be necessary for e.g. analyses similar to the one described in the  
766 present work - not even in the dedicated survival analysis method DegreeCox (Veríssimo, Oliveira, Sagot, &  
767 Vinga, 2016). Using pathway membership information for summarizing cross-pathway linkage was proposed  
768 in (Huttenhower et al., 2009) - however, adjusting its error rate model to other purposes has not been  
769 straightforward.

770 Technically, individual scores that estimate samples' uniqueness as compared to the rest of the collection  
771 can be obtained already from ORA, i.e. from the simplest analysis of dichotomous 2x2 tables applied to  
772 sample-specific gene sets (Tavazoie, Hughes, Campbell, Cho, & Church, 1999), (Drăghici, Khatri, Martins,  
773 Ostermeier, & Krawetz, 2003), (Khatri, Draghici, Ostermeier, & Krawetz, 2002), (Robinson, Grigull,

774 Mohammad, & Hughes, 2002), also called “class I” in the classification by Huang et al.(Huang et al., 2009).  
775 For comparison, the most popular gene set enrichment analysis, GSEA (A. Subramanian et al., 2005) has  
776 been usually applied to finding pathway enrichment in gene lists pre-ranked by cohort-wise statistics. As an  
777 example, Haibe-Kains et al. (Haibe-Kains et al., 2013) analyzed correlations between drug sensitivity and  
778 molecular features calculated on whole *in vitro* drug screens (Barretina et al., 2012),(Garnett et al., 2012)  
779 which are among the datasets re-analyzed in this article. Those pathway enrichment scores represented  
780 correlates of drug sensitivity over the whole screened collections rather than characterized individual cell  
781 lines. Likewise, Iuliano and co-authors (Iuliano, Occhipinti, Angelini, De Feis, & Lió, 2015) matched molecular  
782 landscapes to survival in cancer sample cohorts in order to reverse-engineer relevant pathway and network  
783 structures. Thus, global methods often employ powerful, heavily optimized statistical techniques and are  
784 used for sample exploration or differential expression analysis (Basu et al., 2013), (Yu, Zeng, & Li, 2015) but  
785 cannot serve features for phenotype prediction in novel cell lines or tumors. An overview of network  
786 applications in cancer studies (Y.-A. Kim, Cho, & Przytycka, 2016) showed that, indeed, most of the existing  
787 methods enabled exploratory analyses, discovery of driver genes and pathways as well as splitting a cohort  
788 into molecular subtypes, but did not characterize individual cases.

789 A number of hybrid approaches, such as SPIA (Tarca et al., 2009) and iPAS (Ahn, Lee, Huh, & Park, 2014)  
790 were also capable of calculating sample-specific pathway scores. However, their scores were based on gene  
791 expression values, which excluded the using of other data types. A genuinely integrative multi-omics method  
792 PARADIGM (Vaske et al., 2010) (the program is currently distributed only via a company web portal), on the  
793 contrary, accounted for combinations of events in the chain DNA->mRNA->protein activity. As input, it  
794 required well characterized regulatory relationships – a complete set of which would rarely be available. Also,  
795 similarly to the former group of methods, it relied on comparing cancer to normal samples. Those dramatic  
796 alterations between the normal and cancer tissues encompassing thousands of genes would mask more  
797 fine-grained features that determine between-tumor heterogeneity, differences between sensitive and  
798 refractory cases etc. This requirement also precluded analyzing data where normal matches are missing,  
799 such as the widely used in our analysis cancer cell lines. Finally, EnrichNet (Glaab et al., 2012) has been an  
800 algorithm closest in spirit to NEA: by using random walk with restart (hence not limited to 1-step network  
801 distances), it can trace AGS-FGS relationships via network paths. However it existed only in a single-AGS,  
802 web-based implementation and therefore was also not available for testing it the present analysis.

803 Even though individual enrichment scores can be correlated with phenotypes, they have still been rarely  
804 used in predictor models. In the case of ORA and GSEA, the major reason was that the enrichment is mostly

805 detectable for large FGSs (hundreds to thousands genes), but such are unlikely to characterize functional  
806 differences between tumors - while compact, specific, and discriminatory gene sets tend to escape their  
807 limits of statistical power. Nonetheless, Drier et al. (Drier, Sheffer, & Domany, 2013) have explored cancer  
808 cohorts with pathway-level sample scores derived from gene expression data in a quantitative way and found  
809 that certain sample clusters can be associated with patient survival. On the other hand, the network-based  
810 methods have been developed only recently and are therefore 'too young' to have been exploited fully.  
811 Above, we have also mentioned the network-based regularization of multiple regression models where  
812 inclusion of gene terms into the models was essentially coupled to their co-expression.

813 We finally decided to include in our testing, in parallel with PWNEA (pathway level NEA) and GNEA (gene  
814 node level NEA), the following methods:

- 815 1) Using original gene profiles from respective omics platforms;
- 816 2) ORA, over-representation analysis which was capable of working on exactly the same AGS and FGS  
817 as PWNEA;
- 818 3) GSEA on full ranked gene lists, applying two alternative methods:
  - 819 a. AGSEA, ranking by absolute gene expression value,
  - 820 b. ZGSEA, ranking by deviation of gene expression from the cohort mean;
- 821 4) SPIA, measuring the pathway perturbation via known intra-pathway topology.

822 Using GSEA and SPIA was restricted to only transcriptomics data. SPIA, in addition, could only be run on  
823 pathways with known topology, which limited the set of available FGS to 197 KEGG pathways available in  
824 KGML format. This created an additional, specific line of testing on a limited collection of input data and  
825 FGSs for the methods ORA, AGSEA, ZGSEA, SPIA, and PWNEA (see Fig. 3,4 and Table 3).

## 826 *Network Enrichment Analysis (NEA, PWNEA, and GNEA)*

### 827 **Network**

828 The network was based on the FunCoup method (Andrey Alexeyenko & Sonnhammer, 2009) with  
829 consecutive merging of five more resources as described and benchmarked previously (Merid et al., 2014).  
830 The results of that benchmark indicated that FunCoup was superior to STRING (a method similar to  
831 FunCoup in terms of scale and the size of input data collection, (von Mering et al., 2007)), mostly due to the  
832 latter broadly using prokaryotic evidence and therefore less specific in cancer-related analyses. The second  
833 conclusion from the benchmark was that adding to the FunCoup network edges of curated databases  
834 significantly improved its performance. We therefore added the FunCoup-based network with functional links

835 from KEGG (Kanehisa, Goto, Kawashima, & Nakaya, 2002), CORUM (Ruepp et al., 2007), and PhosphoSite  
836 (Hornbeck et al., 2012), MSigDB transcription factor-related part, (Liberzon et al., 2015)), and an own  
837 reverse-engineered network (Merid et al., 2014). The resulting network thus combined a wide range of  
838 molecular mechanisms, functional relations, and metrics from high-throughput data sets: physical protein-  
839 protein interactions, membership in same protein complex, membership in the same pathway, correlation of  
840 mRNA profiles, correlation of protein abundance values, protein phosphorylation, coherence of GO  
841 annotations, concordance of upstream regulators (transcription factors and miRNAs), co-localization in same  
842 sub-cellular compartments, similarity of phylogenetic profiles etc. It contained 974,427 edges (links) between  
843 19027 nodes (distinct human gene symbols).

#### 844 **Altered gene sets, AGS**

845 Point mutation data (mutation gene sets):

- 846 • `mutations.mgs`: point-mutated genes that proved to be significantly NEA-enriched to either KEGG  
847 pathway set #05200 "Pathways in cancer" or to the full set of point-mutated genes annotated in the  
848 given genome (the approach described by Merid et al. (Merid et al., 2014)).

849 Gene copy number and expression data:

- 850 • `top.200` and `top.400`: genes with copy number or mRNA expression value that in the given  
851 genome was among top 200 or top 400 most deviating from the gene's cohort mean using the one-  
852 sample Z-score. Each AGS thus had a fixed size, regardless of formal significance.
- 853 • `significant`: most deviating from the gene's cohort mean (same as above), but selected only if  
854 below the formal significance threshold (Benjamini-Hochberg (Benjamini & Hochberg, 1995)  
855 adjusted p-value<0.05). These AGSs had variable sizes, depending on the significance criterion.
- 856 • `significant.filtered.mini`: members of the respective `significant` set had, in addition,  
857 to be also significantly NEA-enriched to either KEGG set #05200 "Pathways in cancer" or to  
858 `mutations.mgs` set of the same sample (whichever NEA score passed the significance threshold  
859 NEA FDR=0.05).
- 860 • `significant.filtered.maxi`: members of the respective `significant` set were required to  
861 be significantly NEA-enriched to any of the signaling pathways (including all cancer ones) or to  
862 `mutations.mgs` set of the same sample.

863 Combined (multi-platform) AGS:

864 • `significant.filtered.combined.mini`: a merge of all sets of type

865 `significant.filtered.mini`.

866 • `significant.filtered.combined.maxi`: a merge of all sets of type

867 `significant.filtered.maxi`.

## 868 FGS

869 The functional gene sets, FGSs, were AGS counterparts in the analysis. The main collection of 328 FGS was  
870 based on the KEGG pathways, the full collection of which was complemented with a number of separately  
871 published cancer pathways as well as specific GO terms corresponding to cancer-relevant signaling or  
872 hallmarks of cancer (around 70 cancer- and signaling-related gene sets from Reactome, Gene Ontology,  
873 WikiPathways and literature). Another approach was applied to enable compatibility with GSEA and SPIA.  
874 These methods were designed and are most suitable for analyzing expression data and, apart from that,  
875 SPIA was applicable only to pathways with well characterized intra-pathway topology. We therefore  
876 employed a special set of 197 KEGG pathways for which the topology was available in KGML files and  
877 tested on it SPIA, GSEA, ORA, and PWNEA exclusively gene expression data (these results were separately  
878 labeled as ORA.kegg, SPIA.kegg, AGSEA.kegg, ZGSEA.kegg, and PWNEA.kegg). The analysis on the FGS  
879 collection is referred to as pathway-level NEA (PWNEA).

880 In the other version of our analysis, called gene-wise NEA (GNEA), we treated each of the 19027 network  
881 nodes, regardless of their pathway or GO annotation, as a single-gene FGS.

882

## 883 Method

884 The major principles of NEA were described earlier (Andrey Alexeyenko et al., 2012). In the current  
885 implementation, we evaluated enrichment of AGS versus FGS by the formula:

$$886 \chi^2 = \frac{(n_{\text{AGS-FGS}} - \hat{n}_{\text{AGS-FGS}})^2}{\hat{n}_{\text{AGS-FGS}}} + \frac{(!n_{\text{AGS-FGS}} - !\hat{n}_{\text{AGS-FGS}})^2}{! \hat{n}_{\text{AGS-FGS}}},$$

887 where  $!n$  means “complement to  $n$ ”, i.e. all global network edges that did not belong to  $N_{\text{AGS-FGS}}$ . The number  
888 of links expected under true null, i.e. by chance, was determined by:

$$\hat{n}_{\text{AGS-FGS}} = \frac{N_{\text{AGS}} * N_{\text{FGS}}}{2 * N_{\text{total}}}$$

889 Node connectivity values (numbers of all edges for each given node) were pre-calculated by the algorithm in  
890 advance, given the input network. Then  $N_{\text{AGS}}$  and  $N_{\text{FGS}}$  reported the sums of connectivities of member nodes  
891 of AGS and FGS, respectively, and  $N_{\text{total}}$  was the number of edges in the whole network. Since it was  
892 desirable to provide normally distributed values for the downstream analyses (linear modeling, correlation,  
893 survival), we calculated p-values from the  $X^2$  statistic  $p(H_0)=f(X^2)$  using function `pchisq` available in R  
894 language and then re-calculated corresponding z-scores from the p-values as  $Z=F(p(H_0))$  with function  
895 `qnorm`. Since  $X^2$  is only defined on the non-negative domain, the z-scores were coerced negative in cases of  
896 depletion, i.e. when

$$897 \quad \hat{n}_{\text{AGS-FGS}} > n_{\text{AGS-FGS}} .$$

898 An important feature of GNEA (gene-wise NEA) is that its enrichment estimates are, on average, based on  
899 fewer network edges compared to PWNEA, so that often  $n_{\text{AGS-FGS}} = 0$ . In such cases, the enrichment score  
900 is negative and the difference  $n_{\text{AGS-FGS}} - \hat{n}_{\text{AGS-FGS}}$  reduces to  $-\hat{n}_{\text{AGS-FGS}}$ , which, in its turn, is a function of  
901 cumulative connectivity values  $N_{\text{AGS}}$  and  $N_{\text{FGS}}$ . In other words, lower NEA scores are then assigned to AGS-  
902 FGS pairs with more highly connected member nodes.

903 The steps of NEA described above can be performed with functions available in R package `NEArender`  
904 (<https://cran.r-project.org/web/packages/NEArender/>).

### 905 **Signaling pathway impact analysis, SPIA**

906 The method by Tarca et al. (Tarca et al., 2009) was implemented as an R package `SPIA`. The authors  
907 presented it as combination of two p-values:  $p_{\text{NDE}}$  from common analysis of overrepresentation of  
908 differentially expressed genes in KEGG pathways and  $p_{\text{PERT}}$  from a perturbation analysis by accounting for  
909 topological relations of the same genes within each KEGG pathway. Since the authors claimed that  $p_{\text{NDE}}$   
910 values are no different from p-values from the trivial ORA, we used the pure  $p_{\text{PERT}}$  values from function  
911 `spia` (while the performance of ORA was evaluated separately). In order to get normally distributed values  
912 for our analyses,  $p_{\text{PERT}}$  were transformed to Z-scores and signed according to the SPIA “Activated/inhibited”  
913 status as:

```
914 Z.spia=qnorm(pPERT/2, lower.tail=F)*ifelse(s1$Status=="Activated", 1, -1);
```

## 915 **Gene Set Enrichment Analysis, GSEA**

916 The R implementation of GSEA was downloaded from  
917 [http://software.broadinstitute.org/gsea/msigdb/download\\_file.jsp?filePath=/resources/software/GSEA-P-](http://software.broadinstitute.org/gsea/msigdb/download_file.jsp?filePath=/resources/software/GSEA-P-R.1.0.zip)  
918 [R.1.0.zip](http://software.broadinstitute.org/gsea/msigdb/download_file.jsp?filePath=/resources/software/GSEA-P-R.1.0.zip) (see also [https://software.broadinstitute.org/cancer/software/gsea/wiki/index.php/R-](https://software.broadinstitute.org/cancer/software/gsea/wiki/index.php/R-GSEA_Readme)  
919 [GSEA\\_Readme](https://software.broadinstitute.org/cancer/software/gsea/wiki/index.php/R-GSEA_Readme)). While GSEA possesses a sophisticated toolbox for significance estimation via permutation  
920 tests, we needed only the enrichment score and therefore calculated only the core ES values via function  
921 `GSEA.EnrichmentScore`. Normally, GSEA has been used for analyzing gene rankings from multi-sample  
922 analyses with replicates, such as a *t*-test of an experimental versus control group. The single-sample GSEA  
923 (so called ssGSEA) needed for our analysis was described by Barbie et al. (Barbie et al., 2009). They  
924 produced sample-specific lists by ranking genes by absolute expression values in each given sample. We  
925 implemented this analysis under acronym AGSEA. However this approach might miss sample specificity. As  
926 an example, such ubiquitously expressed genes as GAPDH, RPS16, and RPS11 were found among the top  
927 10 items in more than 90% of the CCLE cell line transcriptomes. For this reason, we additionally  
928 implemented and tested ranking genes in each sample by z-scores, i.e. by the standardized deviations from  
929 the genes' means across the whole cohort. Using this option, dubbed ZGSEA, was similar to `mode_topnorm`  
930 for calculating AGS in function `samples2ags` of our package `NEArender`.

## 931 **Overrepresentation analysis, ORA**

932 The overrepresentation analysis, ORA estimated the significance of overlap between AGS and FGS in 2x2  
933 tables. We did it via Fisher's exact test using the function `gsea.render` in the R package `NEArender`  
934 described above. In order to get ORA values normally distributed, the "estimate" values from function  
935 `fisher.test` were augmented with a pseudo-score 0.1 and log-transformed.

## 936 **Correlation between drug sensitivity and molecular features**

937 In each of the four drug screens, we quantified correlation between the cell line sensitivity to each drug and  
938 each of the molecular features *F* according to a general model of the form:

$$S_d = \beta F + \varepsilon$$

939 where  $\varepsilon$  denotes residual, i.e. unexplained by feature *F*, variance. The features were either original gene  
940 profiles from the three platforms (point mutations screens, copy number arrays, and expression microarrays)  
941 or scores from GSEA, or scores from the two NEA modes, PWNEA and GNEA, i.e. pathway-level network



942 enrichment scores and single-gene network enrichment scores, respectively. All data sets, except the point  
943 mutation set, contained continuous variables and were thus analyzed using Spearman rank correlation. The  
944 point mutation data were analyzed using a one-way ANOVA model with two levels of  $F$ : "any mutation"  
945 versus "wild type". P-values of both Spearman and ANOVA were adjusted by Benjamini and Hochberg  
946 method(Benjamini & Hochberg, 1995).

#### 947 *Elastic net models*

948 Every tested model was built under 10-fold cross-validation using function `cv.glmnet` of R package  
949 `glmnet` ([http://web.stanford.edu/~hastie/glmnet/glmnet\\_alpha.html](http://web.stanford.edu/~hastie/glmnet/glmnet_alpha.html)) with the following parameters:  
950 `lambda.min.ratio=0.01` (the default) and `nlambda=25` (default was 100). Parameter `alpha` varied as  
951 `{0.1; 0.3; 0.5; 0.9; 1.0}`. The reported cross-validated mean error and the number of variables in the model  
952 corresponded to `lambda.1se`, i.e. largest value of `lambda` found within 1 standard error of the minimum  
953 `lambda`. The regression of observed on predicted values was plotted using `lambda.min`.

#### 954 *Drug sensitivity models in TCGA patients*

955 We used the follow-up time profiles for which both status records "relapse/relapse-free" and "dead/alive"  
956 were available, which allowed creating "relapse-free survival" and "overall survival" variables. Depending on  
957 the cancer aggressiveness and chemotherapy type, different timeframes could become informative in the  
958 analysis of the eight TCGA cohorts. The follow-up timeframes were defined as 1/5<sup>th</sup>, 1/2<sup>nd</sup>, and full available  
959 (up to 18 years) intervals.

960 For the analysis reported in "Statistical power to detect correlates of drug sensitivity", we used 42 drugs  
961 which were applied to at least 10 patients in one of the eight cohorts. In Figure 3 we report fractions of  
962 adjusted p-values (FDR) from this analysis calculated by Benjamini and Hochberg. For the analysis of  
963 "agreement between in vitro screen and clinical data" we only considered 14 of the compounds, which were  
964 found in the *in vitro* sets. The p-values from this analysis were Bonferroni-adjusted in the cross-comparisons  
965 between the *in vitro* and clinical results.

966 Matching significance of the drug-feature correlations that had been detected in the cell-line *in vitro* screens  
967 required accounting for multiple clinical variables. Such phenotype covariates as well as drug treatment data  
968 were obtained from TCGA as biotab files via

969 [https://tcga-data.nci.nih.gov/tcgafiles/ftp\\_auth/distro\\_ftpusers/anonymous/tumor\\*/bcr/biotab/clin/](https://tcga-data.nci.nih.gov/tcgafiles/ftp_auth/distro_ftpusers/anonymous/tumor*/bcr/biotab/clin/)

970 In order to measure and probabilistically estimate these effects, we fitted Cox proportional hazards  
971 regression models for every feature versus drug combination. Using all covariates available a cohort (such  
972 as “age at diagnosis”, “year of diagnosis”, “race”, “gender”, “ethnicity”) could result in unrealistically complex  
973 models. We thus included only covariates most likely associated with the disease prognosis, such as tumor  
974 degree, pathological tumor stage, immunohistochemical statuses in BRCA, Gleason score in PRAD,  
975 Karnofsky score in GBM (Suppl. Table 4). Next, we reasoned that when the association “feature - drug  
976 response” truly exists, we should observe it specifically in the patients who did receive the drug in the given  
977 TCGA cohort. Our survival models of the form

$$\log\left(\frac{\lambda(t|C_1 \dots C_k, D, F)}{\lambda_0(t)}\right) = \beta_1 C_1 + \dots + \beta_k C_k + \beta_d D + \beta_f F + \beta_i D * F + \varepsilon$$

978 contained, apart from the covariates  $C_1 \dots C_k$  and the residual term  $\varepsilon$ , main effects “drug”  $D$  and “feature”  $F$  as  
979 well as the interaction term  $D * F$ . A significant main effect of a drug could be interpreted as patients’ benefit in  
980 total and irrespective of the feature value, e.g. regardless of a gene mutation, or a gene expression, or a  
981 NEA-based pathway score. Conversely, a significant feature effect indicated that the feature correlated with  
982 survival directly, i.e. no matter if the drug was administered or not. Finally, significance of the interaction  
983 indicated efficacy of the drug specifically in patients with feature values either above or below a threshold, so  
984 that respective patterns could be explained by neither of the main effects. The interaction term was thus  
985 central for our purpose of detecting drug-feature correlations, whereas the significance of main effects of  
986 “feature” and “drug” was allowed although not required. As an example, a feature may or may not exhibit a  
987 significant correlation with survival in patients who did not receive the drug.

988 All survival analysis results were obtained using R package `survival` (<http://dx.doi.org/10.1007/978-1-4757-3294-8>). In order to estimate significance of the model terms, we used function `coxph` with  
989 continuous feature vectors. However, for visualizing the survival curves (Fig. 6) each feature was binarized at  
990 a cutoff that yielded the lowest p-value for the interaction term. Apart from the interaction model, we also  
991 checked if the p-value and FDR distributions preserved their properties under a unifactorial model. To this  
992 end, sub-cohorts of respective drug-treated patients were included in the survival analysis with the single  
993 main factor “feature”:  
994

$$\log\left(\frac{\lambda(t|C_1 \dots C_k, D, F)}{\lambda_0(t)}\right) = \beta_f F + \varepsilon$$

995

996 **ACKNOWLEDGEMENTS**

997 The authors are grateful for help from National Bioinformatics Infrastructure Sweden (NBIS), the members of  
998 ACT ('Advanced Cancer Therapies') consortium, and acknowledge financial support from Emil och Wera  
999 Kornells Stiftelse, Stockholm County Council, Swedish Cancer Society, Swedish Research Council, and  
1000 Karolinska Institutet. We also recognize the contribution of specimen donors and research groups behind the  
1001 samples of Cancer Cell Line Encyclopedia and The Cancer Genome Atlas.

1002 **COMPETING INTERESTS**

1003 The authors declare that they have no financial and non-financial competing interests.

1004 **REFERENCES**

- 1005 Ahn, T., Lee, E., Huh, N., & Park, T. (2014). Personalized identification of altered pathways in cancer using  
1006 accumulated normal tissue data. *Bioinformatics (Oxford, England)*, *30*(17), i422-429.  
1007 <https://doi.org/10.1093/bioinformatics/btu449>
- 1008 Akahira, J.-I., Aoki, M., Suzuki, T., Moriya, T., Niikura, H., Ito, K., ... Yaegashi, N. (2004). Expression of  
1009 EBAG9/RCA51 is associated with advanced disease in human epithelial ovarian cancer. *British*  
1010 *Journal of Cancer*, *90*(11), 2197–2202. <https://doi.org/10.1038/sj.bjc.6601832>
- 1011 Alcaraz, N., List, M., Batra, R., Vandin, F., Ditzel, H. J., & Baumbach, J. (2017). De novo pathway-based  
1012 biomarker identification. *Nucleic Acids Research*. <https://doi.org/10.1093/nar/gkx642>
- 1013 Alexeyenko, A., Schmitt, T., Tjarnberg, A., Guala, D., Frings, O., & Sonnhammer, E. L. L. (2012). Comparative  
1014 interactomics with Funcoup 2.0. *Nucleic Acids Research*, *40*(D1), D821–D828.  
1015 <https://doi.org/10.1093/nar/gkr1062>
- 1016 Alexeyenko, Andrey, Lee, W., Pernemalm, M., Guegan, J., Dessen, P., Lazar, V., ... Pawitan, Y. (2012). Network  
1017 enrichment analysis: extension of gene-set enrichment analysis to gene networks. *BMC*  
1018 *Bioinformatics*, *13*, 226. <https://doi.org/10.1186/1471-2105-13-226>
- 1019 Alexeyenko, Andrey, & Sonnhammer, E. L. L. (2009). Global networks of functional coupling in eukaryotes  
1020 from comprehensive data integration. *Genome Research*, *19*(6), 1107–1116.  
1021 <https://doi.org/10.1101/gr.087528.108>

- 1022 Barbie, D. A., Tamayo, P., Boehm, J. S., Kim, S. Y., Moody, S. E., Dunn, I. F., ... Hahn, W. C. (2009). Systematic  
1023 RNA interference reveals that oncogenic KRAS-driven cancers require TBK1. *Nature*, *462*(7269),  
1024 108–112. <https://doi.org/10.1038/nature08460>
- 1025 Barretina, J., Caponigro, G., Stransky, N., Venkatesan, K., Margolin, A. A., Kim, S., ... Garraway, L. A. (2012).  
1026 The Cancer Cell Line Encyclopedia enables predictive modelling of anticancer drug sensitivity.  
1027 *Nature*, *483*(7391), 603–607. <https://doi.org/10.1038/nature11003>
- 1028 Basu, A., Bodycombe, N. E., Cheah, J. H., Price, E. V., Liu, K., Schaefer, G. I., ... Schreiber, S. L. (2013). An  
1029 interactive resource to identify cancer genetic and lineage dependencies targeted by small  
1030 molecules. *Cell*, *154*(5), 1151–1161. <https://doi.org/10.1016/j.cell.2013.08.003>
- 1031 Benjamini, Y., & Hochberg, Y. (1995). Controlling the False Discovery Rate: A Practical and Powerful  
1032 Approach to Multiple Testing. *Journal of the Royal Statistical Society. Series B (Methodological)*,  
1033 *57*(1), 289–300.
- 1034 Bittner, L. (1962). R. Bellman, Adaptive Control Processes. A Guided Tour. XVI + 255 S. Princeton, N. J., 1961.  
1035 Princeton University Press. Preis geb. \$ 6.50. *ZAMM - Zeitschrift für Angewandte Mathematik und*  
1036 *Mechanik*, *42*(7–8), 364–365. <https://doi.org/10.1002/zamm.19620420718>
- 1037 Cancer Genome Atlas Research Network. (2008). Comprehensive genomic characterization defines human  
1038 glioblastoma genes and core pathways. *Nature*, *455*(7216), 1061–1068.  
1039 <https://doi.org/10.1038/nature07385>
- 1040 Cheng, W.-Y., Yang, T.-H. O., & Anastassiou, D. (2013). Biomolecular Events in Cancer Revealed by Attractor  
1041 Metagenes. *PLoS Computational Biology*, *9*(2), e1002920.  
1042 <https://doi.org/10.1371/journal.pcbi.1002920>
- 1043 Committee on the Review of Omics-Based Tests for Predicting Patient Outcomes in Clinical Trials, Board on  
1044 Health Care Services, Board on Health Sciences Policy, & Institute of Medicine. (2012). *Evolution of*  
1045 *Translational Omics: Lessons Learned and the Path Forward*. (C. M. Micheel, S. J. Nass, & G. S.  
1046 Omenn, Eds.). Washington (DC): National Academies Press (US). Retrieved from  
1047 <http://www.ncbi.nlm.nih.gov/books/NBK202168/>

- 1048 Costello, J. C., Heiser, L. M., Georgii, E., Gönen, M., Menden, M. P., Wang, N. J., ... Stolovitzky, G. (2014). A  
1049 community effort to assess and improve drug sensitivity prediction algorithms. *Nature*  
1050 *Biotechnology*, 32(12), 1202–1212. <https://doi.org/10.1038/nbt.2877>
- 1051 Crystal, A. S., Shaw, A. T., Sequist, L. V., Friboulet, L., Niederst, M. J., Lockerman, E. L., ... Engelman, J. A.  
1052 (2014). Patient-derived models of acquired resistance can identify effective drug combinations for  
1053 cancer. *Science*, 346(6216), 1480–1486. <https://doi.org/10.1126/science.1254721>
- 1054 Dirmeier, S., Fuchs, C., Mueller, N. S., & Theis, F. J. (2017). netReg: network-regularized linear models for  
1055 biological association studies. *Bioinformatics*. <https://doi.org/10.1093/bioinformatics/btx677>
- 1056 Domcke, S., Sinha, R., Levine, D. A., Sander, C., & Schultz, N. (2013). Evaluating cell lines as tumour models  
1057 by comparison of genomic profiles. *Nature Communications*, 4.  
1058 <https://doi.org/10.1038/ncomms3126>
- 1059 Drăghici, S., Khatri, P., Martins, R. P., Ostermeier, G. C., & Krawetz, S. A. (2003). Global functional profiling of  
1060 gene expression. *Genomics*, 81(2), 98–104. [https://doi.org/10.1016/S0888-7543\(02\)00021-6](https://doi.org/10.1016/S0888-7543(02)00021-6)
- 1061 Drier, Y., Sheffer, M., & Domany, E. (2013). Pathway-based personalized analysis of cancer. *Proceedings of*  
1062 *the National Academy of Sciences*, 110(16), 6388–6393. <https://doi.org/10.1073/pnas.1219651110>
- 1063 Forbes, S. A., Beare, D., Gunasekaran, P., Leung, K., Bindal, N., Boutselakis, H., ... Campbell, P. J. (2014).  
1064 COSMIC: exploring the world's knowledge of somatic mutations in human cancer. *Nucleic Acids*  
1065 *Research*. <https://doi.org/10.1093/nar/gku1075>
- 1066 Friedman, J., Hastie, T., & Tibshirani, R. (2010). Regularization Paths for Generalized Linear Models via  
1067 Coordinate Descent. *Journal of Statistical Software*, 33(1). <https://doi.org/10.18637/jss.v033.i01>
- 1068 Garnett, M. J., Edelman, E. J., Heidorn, S. J., Greenman, C. D., Dastur, A., Lau, K. W., ... Benes, C. H. (2012).  
1069 Systematic identification of genomic markers of drug sensitivity in cancer cells. *Nature*, 483(7391),  
1070 570–575. <https://doi.org/10.1038/nature11005>
- 1071 Giatromanolaki, A., Sivridis, E., Maltezos, E., & Koukourakis, M. I. (2002). Down-regulation of intestinal-type  
1072 alkaline phosphatase in the tumor vasculature and stroma provides a strong basis for explaining  
1073 amifostine selectivity. *Seminars in Oncology*, 29(6 Suppl 19), 14–21.  
1074 <https://doi.org/10.1053/sonc.2002.37356>

- 1075 Glaab, E., Baudot, A., Krasnogor, N., Schneider, R., & Valencia, A. (2012). EnrichNet: network-based gene set  
1076 enrichment analysis. *Bioinformatics (Oxford, England)*, *28*(18), i451–i457.  
1077 <https://doi.org/10.1093/bioinformatics/bts389>
- 1078 Haibe-Kains, B., El-Hachem, N., Birkbak, N. J., Jin, A. C., Beck, A. H., Aerts, H. J. W. L., & Quackenbush, J.  
1079 (2013). Inconsistency in large pharmacogenomic studies. *Nature*, *504*(7480), 389–393.  
1080 <https://doi.org/10.1038/nature12831>
- 1081 Heng, H. H. (2015). *Debating Cancer: The Paradox in Cancer Research*. World Scientific.
- 1082 Hornbeck, P. V., Kornhauser, J. M., Tkachev, S., Zhang, B., Skrzypek, E., Murray, B., ... Sullivan, M. (2012).  
1083 PhosphoSitePlus: a comprehensive resource for investigating the structure and function of  
1084 experimentally determined post-translational modifications in man and mouse. *Nucleic Acids  
1085 Research*, *40*(D1), D261–D270. <https://doi.org/10.1093/nar/gkr1122>
- 1086 Huang, D. W., Sherman, B. T., & Lempicki, R. A. (2009). Bioinformatics enrichment tools: paths toward the  
1087 comprehensive functional analysis of large gene lists. *Nucleic Acids Research*, *37*(1), 1–13.  
1088 <https://doi.org/10.1093/nar/gkn923>
- 1089 Huttenhower, C., Haley, E. M., Hibbs, M. A., Dumeaux, V., Barrett, D. R., Collier, H. A., & Troyanskaya, O. G.  
1090 (2009). Exploring the human genome with functional maps. *Genome Research*, *19*(6), 1093–1106.  
1091 <https://doi.org/10.1101/gr.082214.108>
- 1092 Iorio, F., Knijnenburg, T. A., Vis, D. J., Bignell, G. R., Menden, M. P., Schubert, M., ... Garnett, M. J. (2016). A  
1093 Landscape of Pharmacogenomic Interactions in Cancer. *Cell*, *166*(3), 740–754.  
1094 <https://doi.org/10.1016/j.cell.2016.06.017>
- 1095 Iuliano, A., Occhipinti, A., Angelini, C., De Feis, I., & Lió, P. (2015). Applications of Network-based Survival  
1096 Analysis Methods for Pathways Detection in Cancer. In C. di Serio, P. Liò, A. Nonis, & R. Tagliaferri  
1097 (Eds.), *Computational Intelligence Methods for Bioinformatics and Biostatistics* (Vol. 8623, pp. 76–  
1098 88). Cham: Springer International Publishing. Retrieved from [http://link.springer.com/10.1007/978-  
1099 3-319-24462-4\\_7](http://link.springer.com/10.1007/978-3-319-24462-4_7)

- 1100 Jeggari, A., & Alexeyenko, A. (2017). NEArrender: an R package for functional interpretation of ‘omics’ data  
1101 via network enrichment analysis. *BMC Bioinformatics*, 18(S5). <https://doi.org/10.1186/s12859-017->  
1102 1534-y
- 1103 Kanehisa, M., Goto, S., Kawashima, S., & Nakaya, A. (2002). The KEGG databases at GenomeNet. *Nucleic*  
1104 *Acids Research*, 30(1), 42–46.
- 1105 Khatri, P., Draghici, S., Ostermeier, G. C., & Krawetz, S. A. (2002). Profiling Gene Expression Using Onto-  
1106 Express. *Genomics*, 79(2), 266–270. <https://doi.org/10.1006/geno.2002.6698>
- 1107 Kim, S., Pan, W., & Shen, X. (2013). Network-based penalized regression with application to genomic data.  
1108 *Biometrics*, 69(3), 582–593. <https://doi.org/10.1111/biom.12035>
- 1109 Kim, Y.-A., Cho, D.-Y., & Przytycka, T. M. (2016). Understanding Genotype-Phenotype Effects in Cancer via  
1110 Network Approaches. *PLOS Computational Biology*, 12(3), e1004747.  
1111 <https://doi.org/10.1371/journal.pcbi.1004747>
- 1112 Kurnit, K. C., Bailey, A. M., Zeng, J., Johnson, A. M., Shufean, M. A., Brusco, L., ... Meric-Bernstam, F. (2017).  
1113 “Personalized Cancer Therapy”: A Publicly Available Precision Oncology Resource. *Cancer Research*,  
1114 77(21), e123–e126. <https://doi.org/10.1158/0008-5472.CAN-17-0341>
- 1115 Laupacis, A., Sackett, D. L., & Roberts, R. S. (1988). An Assessment of Clinically Useful Measures of the  
1116 Consequences of Treatment. *New England Journal of Medicine*, 318(26), 1728–1733.  
1117 <https://doi.org/10.1056/NEJM198806303182605>
- 1118 Lee, W., Alexeyenko, A., Pernemalm, M., Guegan, J., Dessen, P., Lazar, V., ... Pawitan, Y. (2015). Identifying  
1119 and Assessing Interesting Subgroups in a Heterogeneous Population. *BioMed Research*  
1120 *International*, 2015, 462549. <https://doi.org/10.1155/2015/462549>
- 1121 Li, C., & Li, H. (2008). Network-constrained regularization and variable selection for analysis of genomic  
1122 data. *Bioinformatics*, 24(9), 1175–1182. <https://doi.org/10.1093/bioinformatics/btn081>
- 1123 Liberzon, A., Birger, C., Thorvaldsdóttir, H., Ghandi, M., Mesirov, J. P., & Tamayo, P. (2015). The Molecular  
1124 Signatures Database (MSigDB) hallmark gene set collection. *Cell Systems*, 1(6), 417–425.  
1125 <https://doi.org/10.1016/j.cels.2015.12.004>

- 1126 Margolin, A. A., Bilal, E., Huang, E., Norman, T. C., Ottestad, L., Mecham, B. H., ... Børresen-Dale, A.-L.  
1127 (2013). Systematic analysis of challenge-driven improvements in molecular prognostic models for  
1128 breast cancer. *Science Translational Medicine*, 5(181), 181re1.  
1129 <https://doi.org/10.1126/scitranslmed.3006112>
- 1130 Maslov, S., & Sneppen, K. (2002). Specificity and stability in topology of protein networks. *Science (New*  
1131 *York, N.Y.)*, 296(5569), 910–913. <https://doi.org/10.1126/science.1065103>
- 1132 Merid, S. K., Goranskaya, D., & Alexeyenko, A. (2014). Distinguishing between driver and passenger  
1133 mutations in individual cancer genomes by network enrichment analysis. *BMC Bioinformatics*, 15,  
1134 308. <https://doi.org/10.1186/1471-2105-15-308>
- 1135 Parker, J. S., Mullins, M., Cheang, M. C. U., Leung, S., Voduc, D., Vickery, T., ... Bernard, P. S. (2009).  
1136 Supervised Risk Predictor of Breast Cancer Based on Intrinsic Subtypes. *Journal of Clinical Oncology*,  
1137 27(8), 1160–1167. <https://doi.org/10.1200/JCO.2008.18.1370>
- 1138 Pogribny, I. P., Dreval, K., Kindrat, I., Melnyk, S., Jimenez, L., de Conti, A., ... Beland, F. A. (2017).  
1139 Epigenetically mediated inhibition of S-adenosylhomocysteine hydrolase and the associated  
1140 dysregulation of 1-carbon metabolism in nonalcoholic steatohepatitis and hepatocellular  
1141 carcinoma. *FASEB Journal: Official Publication of the Federation of American Societies for*  
1142 *Experimental Biology*. <https://doi.org/10.1096/fj.201700866R>
- 1143 Pratt, S. E., Durland-Busbice, S., Shepard, R. L., Heinz-Taheny, K., Iversen, P. W., & Dantzig, A. H. (2013).  
1144 Human Carboxylesterase-2 Hydrolyzes the Prodrug of Gemcitabine (LY2334737) and Confers  
1145 Prodrug Sensitivity to Cancer Cells. *Clinical Cancer Research*, 19(5), 1159–1168.  
1146 <https://doi.org/10.1158/1078-0432.CCR-12-1184>
- 1147 Rajagopalan, P. T. R., Zhang, Z., McCourt, L., Dwyer, M., Benkovic, S. J., & Hammes, G. G. (2002). Interaction  
1148 of dihydrofolate reductase with methotrexate: Ensemble and single-molecule kinetics. *Proceedings*  
1149 *of the National Academy of Sciences of the United States of America*, 99(21), 13481–13486.  
1150 <https://doi.org/10.1073/pnas.172501499>
- 1151 Ritz, C., Baty, F., Streibig, J. C., & Gerhard, D. (2015). Dose-Response Analysis Using R. *PLOS ONE*, 10(12),  
1152 e0146021. <https://doi.org/10.1371/journal.pone.0146021>



- 1153 Robert A. Fisher. (1925). *Statistical methods for research workers*. Edinburgh: Oliver and Boyd.
- 1154 Robinson, M. D., Grigull, J., Mohammad, N., & Hughes, T. R. (2002). FunSpec: a web-based cluster  
1155 interpreter for yeast. *BMC Bioinformatics*, 3, 35.
- 1156 Roepman, P., Jassem, J., Smit, E. F., Muley, T., Niklinski, J., van de Velde, T., ... van Zandwijk, N. (2009). An  
1157 immune response enriched 72-gene prognostic profile for early-stage non-small-cell lung cancer.  
1158 *Clinical Cancer Research: An Official Journal of the American Association for Cancer Research*, 15(1),  
1159 284–290. <https://doi.org/10.1158/1078-0432.CCR-08-1258>
- 1160 Ruepp, A., Brauner, B., Dunger-Kaltenbach, I., Frishman, G., Montrone, C., Stransky, M., ... Mewes, H. W.  
1161 (2007). CORUM: the comprehensive resource of mammalian protein complexes. *Nucleic Acids*  
1162 *Research*, 36(Database), D646–D650. <https://doi.org/10.1093/nar/gkm936>
- 1163 Saxena, M., & Yeretssian, G. (2014). NOD-Like Receptors: Master Regulators of Inflammation and Cancer.  
1164 *Frontiers in Immunology*, 5, 327. <https://doi.org/10.3389/fimmu.2014.00327>
- 1165 Seashore-Ludlow, B., Rees, M. G., Cheah, J. H., Cokol, M., Price, E. V., Coletti, M. E., ... Schreiber, S. L. (2015).  
1166 Harnessing Connectivity in a Large-Scale Small-Molecule Sensitivity Dataset. *Cancer Discovery*,  
1167 5(11), 1210–1223. <https://doi.org/10.1158/2159-8290.CD-15-0235>
- 1168 Shin, J., Carr, A., Corner, G. A., Togel, L., Davaos-Salas, M., Tran, H., ... Mariadason, J. M. (2014). The  
1169 Intestinal Epithelial Cell Differentiation Marker Intestinal Alkaline Phosphatase (ALPi) Is Selectively  
1170 Induced by Histone Deacetylase Inhibitors (HDACi) in Colon Cancer Cells in a Kruppel-like Factor 5  
1171 (KLF5)-dependent Manner. *Journal of Biological Chemistry*, 289(36), 25306–25316.  
1172 <https://doi.org/10.1074/jbc.M114.557546>
- 1173 Shojaie, A., & Michailidis, G. (2010). Network enrichment analysis in complex experiments. *Statistical*  
1174 *Applications in Genetics and Molecular Biology*, 9, Article22. [https://doi.org/10.2202/1544-](https://doi.org/10.2202/1544-6115.1483)  
1175 6115.1483
- 1176 Snijders, A. M., Hermsen, M. A., Baughman, J., Buffart, T. E., Huey, B., Gajduskova, P., ... Albertson, D. G.  
1177 (2008). Acquired genomic aberrations associated with methotrexate resistance vary with  
1178 background genomic instability. *Genes, Chromosomes & Cancer*, 47(1), 71–83.  
1179 <https://doi.org/10.1002/gcc.20509>

- 1180 Storey, J. D., & Tibshirani, R. (2003). Statistical significance for genomewide studies. *Proceedings of the*  
1181 *National Academy of Sciences of the United States of America*, 100(16), 9440–9445.  
1182 <https://doi.org/10.1073/pnas.1530509100>
- 1183 Stransky, N., Ghandi, M., Kryukov, G. V., Garraway, L. A., Lehár, J., Liu, M., ... Saez-Rodriguez, J. (2015).  
1184 Pharmacogenomic agreement between two cancer cell line data sets. *Nature*.  
1185 <https://doi.org/10.1038/nature15736>
- 1186 Subramanian, A., Tamayo, P., Mootha, V. K., Mukherjee, S., Ebert, B. L., Gillette, M. A., ... Mesirov, J. P.  
1187 (2005). Gene set enrichment analysis: A knowledge-based approach for interpreting genome-wide  
1188 expression profiles. *Proceedings of the National Academy of Sciences*, 102(43), 15545–15550.  
1189 <https://doi.org/10.1073/pnas.0506580102>
- 1190 Subramanian, J., & Simon, R. (2010). Gene expression-based prognostic signatures in lung cancer: ready for  
1191 clinical use? *Journal of the National Cancer Institute*, 102(7), 464–474.  
1192 <https://doi.org/10.1093/jnci/djq025>
- 1193 Tabor, H., & Wyngarden, L. (1959). The enzymatic formation of formiminotetrahydrofolic acid, 5,10-  
1194 methenyltetrahydrofolic acid, and 10-formyltetrahydrofolic acid in the metabolism of  
1195 formiminoglutamic acid. *The Journal of Biological Chemistry*, 234(7), 1830–1846.
- 1196 Tarca, A. L., Draghici, S., Khatri, P., Hassan, S. S., Mittal, P., Kim, J. -s., ... Romero, R. (2009). A novel signaling  
1197 pathway impact analysis. *Bioinformatics*, 25(1), 75–82.  
1198 <https://doi.org/10.1093/bioinformatics/btn577>
- 1199 Tavazoie, S., Hughes, J. D., Campbell, M. J., Cho, R. J., & Church, G. M. (1999). Systematic determination of  
1200 genetic network architecture. *Nature Genetics*, 22(3), 281–285. <https://doi.org/10.1038/10343>
- 1201 Vaske, C. J., Benz, S. C., Sanborn, J. Z., Earl, D., Szeto, C., Zhu, J., ... Stuart, J. M. (2010). Inference of patient-  
1202 specific pathway activities from multi-dimensional cancer genomics data using PARADIGM.  
1203 *Bioinformatics*, 26(12), i237–i245. <https://doi.org/10.1093/bioinformatics/btq182>
- 1204 Veríssimo, A., Oliveira, A. L., Sagot, M.-F., & Vinga, S. (2016). DegreeCox – a network-based regularization  
1205 method for survival analysis. *BMC Bioinformatics*, 17(S16), 109–121.  
1206 <https://doi.org/10.1186/s12859-016-1310-4>

- 1207 von Mering, C., Jensen, L. J., Kuhn, M., Chaffron, S., Doerks, T., Krüger, B., ... Bork, P. (2007). STRING 7--  
1208 recent developments in the integration and prediction of protein interactions. *Nucleic Acids*  
1209 *Research*, 35(Database issue), D358-362. <https://doi.org/10.1093/nar/gkl825>
- 1210 Waldron, L., Haibe-Kains, B., Culhane, A. C., Riester, M., Ding, J., Wang, X. V., ... Parmigiani, G. (2014).  
1211 Comparative Meta-analysis of Prognostic Gene Signatures for Late-Stage Ovarian Cancer. *JNCI*  
1212 *Journal of the National Cancer Institute*. <https://doi.org/10.1093/jnci/dju049>
- 1213 Wang, Y., Klijn, J. G. M., Zhang, Y., Sieuwerts, A. M., Look, M. P., Yang, F., ... Foekens, J. A. (2005). Gene-  
1214 expression profiles to predict distant metastasis of lymph-node-negative primary breast cancer.  
1215 *Lancet (London, England)*, 365(9460), 671–679. [https://doi.org/10.1016/S0140-6736\(05\)17947-1](https://doi.org/10.1016/S0140-6736(05)17947-1)
- 1216 Wilk, M. B., & Gnanadesikan, R. (1968). Probability plotting methods for the analysis for the analysis of data.  
1217 *Biometrika*, 55(1), 1–17. <https://doi.org/10.1093/biomet/55.1.1>
- 1218 Williams, E. T., Bacon, J. A., Bender, D. M., Lowinger, J. J., Guo, W.-K., Ehsani, M. E., ... Perkins, E. J. (2011).  
1219 Characterization of the Expression and Activity of Carboxylesterases 1 and 2 from the Beagle Dog,  
1220 Cynomolgus Monkey, and Human. *Drug Metabolism and Disposition*, 39(12), 2305–2313.  
1221 <https://doi.org/10.1124/dmd.111.041335>
- 1222 Yu, X., Zeng, T., & Li, G. (2015). Integrative enrichment analysis: a new computational method to detect  
1223 dysregulated pathways in heterogeneous samples. *BMC Genomics*, 16(1).  
1224 <https://doi.org/10.1186/s12864-015-2188-7>
- 1225 Zhao, S., & Shojaie, A. (2016). A Significance Test for Graph-Constrained Estimation. *Biometrics*, 72(2), 484–  
1226 493. <https://doi.org/10.1111/biom.12418>
- 1227
- 1228

1229 SUPPLEMENTARY FILES

File	Description
SupplementaryTablesAndFigures.docx	Supplementary tables and figures
IC50values.ACTscreen.xlsx	IC50 values of drug sensitivity over the cancer cell lines in the ACT drug screen (see Methods).
glmnetModels.Basu_vs_new.raw.pdf	<p>Building and validation of multivariate models of drug resistance from original point mutation and gene expression data.</p> <p>As explained in Methods, the multivariate models were obtained using the elastic net algorithm under variable 'alpha' parameters (see values A=0.1; A=0.3; A=0.5; A=0.9; A=1 in the top left corners of each page). The algorithm tried to minimize the mean-squared error by reducing the number of features in the model (top legend in upper right plot). The final number of features as well as the 'lambda.1se' at which the practically best performance was achieved are indicated as 'N=' and 'L=' in the top left corner. The right and left vertical dotted lines show absolute minimum lambda and 'lambda.1se' found within 1 standard error of the former, respectively. The chosen features with their linear coefficients are listed below (sorted by coefficient values; the lists are truncated when too long).</p> <p>The two bottom plots display model performance by matching drug sensitivity predicted for each cell line (X axes) on data used for training (blue points, left) and on newly obtained data from the ACT screen (green points, right). The model performance is measured with Spearman rank correlation between predicted and observed data points.</p> <p style="text-align: center;">See also the legend to Figure 5.</p>
glmnetModels.Basu_vs_new.pwnea.pdf	<p>Building and validation of multivariate models of drug resistance from PWNEA scores obtained by using point mutation and gene expression data.</p> <p style="text-align: center;">See the legend above.</p>

1230

1231